

Poster Abstracts: Clinical MRI—Non-ischemic Acquired Heart Disease

319. Cardiovascular Magnetic Resonance Evaluation of Tako-Tsubo Cardiomyopathy

Anastasios Athanasiadis, MD, Marcus Honold, MD, Claudio Kupfahl, MD, Christine Goedecke, MD, Heiko Mahrholdt, MD, Udo Sechtem, MD. *Cardiology, Robert Bosch Medical Center, Stuttgart, Germany.*

Introduction: Tako-Tsubo cardiomyopathy has been reported in Japan and is characterized by transient left ventricular (LV) apical ballooning and reversible LV asynergy in the absence of significant coronary artery disease. This syndrome usually presents clinically as acute myocardial infarction (MI). However, in contrast to acute MI, Tako-Tsubo cardiomyopathy has a benign outcome with full recovery of wall motion within a few weeks and therefore does not require thrombolytic treatment or angioplasty.

Methods and Results: Gd-enhanced contrast CMR is well established for the detection of acute and chronic ischemic myocardial injury and may thus permit a differentiation between Tako-Tsubo cardiomyopathy and acute MI in the acute setting. Contrast CMR imaging using an IR FLASH technique (constantly adapting TI to null normal myocardium) was performed in 11 patients (mean age 66+7 yrs.) presenting with typical apical LV ballooning, LV asynergy and normal coronary arteries, in average three days after cardiac catheterization. In 10 of the 11 patients no contrast enhancement was present. One patient showed evidence of a small myocardial damage in the inferior apical region which morphologically looked like coronary embolism of a side branch in the circumflex region. Acute or chronic myocarditis as possible cause for the transient wall motion abnormality has been ruled out by endomyocardial biopsy in all patients (Fig. 1).

Conclusions: Tako-Tsubo cardiomyopathy is not an exclusively Japanese phenomenon. It is also present in Europe and therefore must be differentiated from acute myocardial infarction in the clinical routine. Contrast CMR is a valuable tool for the non-invasive differentiation of those disease entities in the acute phase and may be useful for therapeutic decision making.

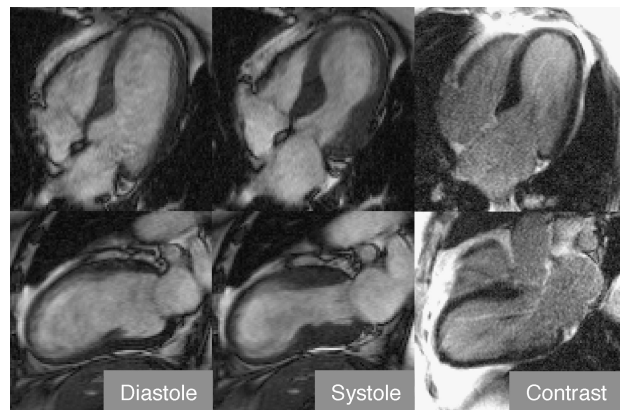


Figure 1.

320. CMR Estimation of Filling Pressures in Left Ventricular Hypertrophy: A Comparison with Tissue Doppler and Invasive Measurements

Bernard P. Paelinck,¹ Hildo J. Lamb,² Jeroen J. Bax,³ Rob J. van der Geest,² Paul M. Parizel,⁴ Christiaan J. Vrints,¹ Albert de Roos.² ¹Cardiology, University Hospital Antwerp, Edegem, Belgium, ²Radiology, LUMC, Leiden, Netherlands, ³Cardiology, LUMC, Leiden, Netherlands, ⁴Radiology, University Hospital Antwerp, Edegem, Belgium.

Introduction: The diastolic long axis displacement velocities of the mitral annulus provide a better estimate of filling pressures as compared to analysis of the mitral inflow velocity curve alone. Phase-contrast cardiovascular magnetic resonance (CMR) allows velocity encoding of both moving structures and blood.

Purpose: We sought to assess if CMR could estimate filling pressures by combining early diastolic mitral annular velocity (Ea) and early (E) mitral velocity.

Methods: 18 patients with hypertensive heart disease (mass index: 114 ± 21 g/m²) and normal or mildly reduced systolic function (left ventricular ejection fraction: $57.6 \pm 6.5\%$) referred for cardiac catheterization underwent consecutive measurement of mitral inflow and mitral annular velocities with Doppler and phase-contrast CMR. These data were compared with mean pulmonary wedge pressure.

Results: The ratio of early mitral flow velocity to early diastolic velocity of the mitral annulus (E/Ea) showed a good correlation between Doppler and CMR phase-contrast ($r=0.89$). $E/Ea < 8$ predicted normal and $E/Ea > 15$ increased mean pulmonary wedge pressure. Between 8 and 15 both techniques displayed a similar variability in predicting mean pulmonary wedge pressure.

Conclusions: Phase-contrast CMR of mitral inflow and diastolic mitral annular motion allows a good estimate of left ventricular filling pressure.

321. Late Enhancement Without Infarction—Appearance and Etiology of Myocardial Late Enhancement in Contrast-Enhanced MRI of Non-ischemic Heart Disease

Peter Hunold, MD,¹ Thomas W. Schlosser, MD,¹ Kai-Uwe Waltering, MD,¹ Sandra Massing, RT,¹ Markus Jochims, MD,² Walter O. Schöler, MD,² Jörg F. Debatin, MD,¹ Jörg Barkhausen, MD.¹ ¹Department for Diagnostic and Interventional Radiology, University Hospital, Essen, Germany, ²Department of Cardiology, Elisabeth Hospital, Essen, Germany.

Introduction: “Late enhancement” (LE) in contrast-enhanced cardiac MRI is currently being established for the assessment of myocardial viability in ischemic heart disease. The region area of enhancement after administration of Gd-based contrast material reflects irreversible damage after chronic myocardial infarction.

Whereas LE is very highly sensitive in detecting myocardial scarring, it is not specific for ischemic damage since Gd-DTPA generally accumulates in

tissues with increased water content. Thus, LE occurs in myocardial areas of fibrosis, inflammation, and edema where the extracellular volume is enlarged. Different myocardial disorders are accompanied by fibrosis or inflammation and might be diagnosed and distinguished from ischemic disease based on the pattern and localization of LE.

Purpose: To summarize and characterize different myocardial disorders presenting with “late enhancement” (LE) in contrast-enhanced MRI, which are not related to acute or chronic myocardial infarction.

Methods: Within 18 months, 811 contrast-enhanced cardiac MRI studies were performed for various indications in the University and an affiliated hospital. All MRI exams were performed on a 1.5 T scanner (Magnetom Sonata, Siemens Medical Systems, Erlangen, Germany). After completion of a cine study, LE scans were acquired 8–15 min after administration of 0.2 mmol/kg BW of Gd-DTPA (Magnevist™, Schering, Berlin, Germany) using an inversion-recovery turboFLASH sequence (TR, 8 ms; TE, 4 ms; flip angle, 25°; TI, 200–260 ms). The entire left ventricular myocardium was covered by long axis and contiguous short axis scans (slice thickness, 8 mm). All data sets were reviewed for myocardial LE. In patients with excluded myocardial infarction, the different causes of LE were assessed, and the different patterns of LE were related to the underlying pathology.

Results: A total of 422 (52%) patients revealed myocardial LE. In 403 (96%) patients with proven CAD and/or a history of myocardial infarction, the transmural extent of LE was variable but always included the subendocardial layer. In 19 patients with angiographically excluded CAD and without a history of myocardial infarction, LE was found due to different diseases: myocarditis (n=4), sarcoidosis (2), left ventricular involvement of arrhythmogenic right ventricular cardiomyopathy (2), hypertrophic cardiomyopathy (4), dilative cardiomyopathy (1), endomyocardial fibrosis (2), small septal fibrosis of unknown origin (1), and iatrogenic scars after endomyocardial biopsy (1), transcatheter ablation of septal hypertrophy (1), and percutaneous myocardial LASER revascularization (1).

Conclusions: All patients with a history of myocardial infarction revealed LE always including the subendocardial layer of the myocardium. However, many non-ischemic cardiac diseases are accompanied by fibrosis or edema and, therefore, provide LE also. If the subendocardial layer is spared out, LE shows a patchy appearance, or there is no evidence of myocardial infarction, different myocardial diseases must be considered as a differential diagnosis when myocardial LE appears. On the other hand, performing LE imaging



might facilitate the differential diagnosis in non-ischemic heart disease.

322. Asynchronous Regional Myocardial Contraction in LBBB in Relation to Ejection and Iso-Volumic-Relaxation-Times Assessed by High Temporal Resolution MR Tissue Tagging

Marco J. W. Gotte, MD, PhD,¹ Jaco J. M. Zwanenburg, Msc,² Willem G. van Dockum, MD,¹ Paul Knaapen, MD,¹ J. Tim Marcus, PhD,² Albert C. van Rossum, MD, PhD.¹ ¹Cardiology, Vrije Universiteit Medical Center, Amsterdam, Netherlands, ²Department of Physics & Medical Technology, Vrije Universiteit Medical Center, Amsterdam, Netherlands.

Introduction: Recent studies have shown that the presence of a left bundle branch block (LBBB) prolongs overall myocardial tension and reduces filing times (Grines et al., 1989; Xiao et al., 1991). In order to study how regional asynchrony is related with ejection and iso-volumic-relaxation-times, high temporal resolution myocardial tagging was applied to evaluate cardiac contraction in patients with a LBBB.

Purpose: To map regional mechanical activity of the left ventricle in patients with a LBBB and related this to the time of aortic valve closure (Tavc) and iso-volumic-relaxation time (IVRT).

Methods: Patients: Ten patients (8 males, age 56±13 years) with a LBBB (QRS 146±39ms) and depressed LV function (EF<45%, NYHA class III) were studied. Imaging: Five consecutive short-axis tagged image planes with high temporal resolution (14 ms) were acquired using steady state free precession (SSFP) imaging

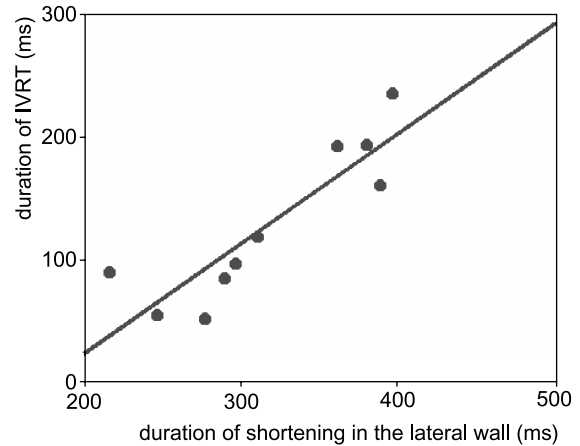


Figure 2. (View this art in color at www.dekker.com.)

(Zwanenburg et al., 2003) and a multiple breath-hold scheme. A three-chamber cine image with the same high temporal resolution was used to determine the T_{avc} and mitral valve opening (T_{mvo}) relative to the ECG-R wave. T_{avc} marked the end of the ejection period. The IVRT was calculated as (T_{mvo}-T_{avc}). Post-processing: Circumferential strain (ε_c) curves were calculated using HARP (Osman et al., 1998) and averaged for 6 segments per slice: infero-septal (IS), antero-septal (AS), anterior (AN), antero-lateral (AL), postero-lateral (PL) and inferior (IN). The time to onset of shortening (T_{os}) relative to the ECG-R wave was defined as the beginning of the down slope of the ε_c curve and assessed by an automatic fitting algorithm. From the strain curves, the maximum circumferential shortening (CS_{peak}) and the time to peak shortening (T_{peakCS}) were obtained.

Results: The averaged onset time of shortening for each segment is shown in Figure 1. Onset of shortening in the lateral wall (AL+PL) started significantly later compared to the septum (IS+AS), 99±21 ms vs. 65±34 ms, respectively, p<0.02). There was no difference in T_{os} between the AN and IN regions. Shortening started earlier at the apex compared to base (79±21 ms vs. 100±17 ms, p<0.05). The CS_{peak} was significantly reduced in the septum compared to the lateral wall (5±2% vs. 13±4%, p<0.001). CS_{peak} was not different between AN and IN, and between apex and base.

Peak shortening was reached significantly later in the lateral wall compared to the septum (415±73 ms vs. 219±105 ms, p<0.001). No differences in T_{peakCS} were found between AN and IN, and between apex and base. The T_{peakCS} in the lateral wall was significantly later than the T_{avc} (370±57 ms, p<0.02), indicating post-systolic shortening. Duration of contraction was found to be the longest in the lateral wall (316±63 ms). It was found that the duration of the IVRT was

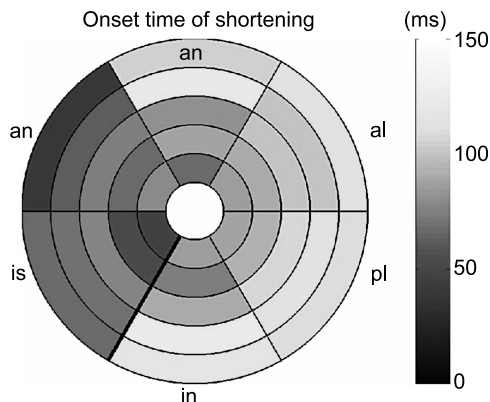


Figure 1. (View this art in color at www.dekker.com.)



highly correlated to the duration of contraction in this region (AL+PL) ($r=0.88$, $p=0.001$, Figure 2).

Conclusion: In patients with a LBBB, onset of circumferential shortening starts in the septal and apical regions and propagates to the lateral and basal regions. Delayed onset of shortening in the lateral wall is accompanied by a longer duration of shortening resulting in post-systolic shortening and prolonged duration of IVRT. Therefore, a LBBB prolongs ventricular contraction at the lateral wall disproportionate to the ejection time, and simultaneously reduces the filling period.

Acknowledgment: Supported by the Netherlands Heart Foundation, grant 2000B220.

REFERENCES

Grines, C. L., Bashore, T. M., Boudoulas, H., et al. (1989). *Circulation* 79:845–853.

Osman, N. F., Prince, J. L. (1998). *Proc. SPIE Med. Imag. Conf. San Diego*, 142–152.

Xiao, H. B., Lee, C. H., Gibson, D. G. (1991). *Br. Heart J.* 66:443–447.

Zwanenburg, J. J. M., Kuijper, J. P. A., et al. (2003). *Magn. Reson. Med.* 49:722–730.

323. The Normal Physiological Variation of Left Ventricular Mass, Dimensions, and Function from Childhood to Late Adulthood by MRI: A Prospective Study of 102 Healthy Volunteers Age 12–81 Years

Peter Cain, MD, PHD, Ragnhild Ahl, MD, Erik Hedstrom, Hakan Arheden, MD, PHD. *Department of Physiology, University of Lund, Lund, Sweden.*

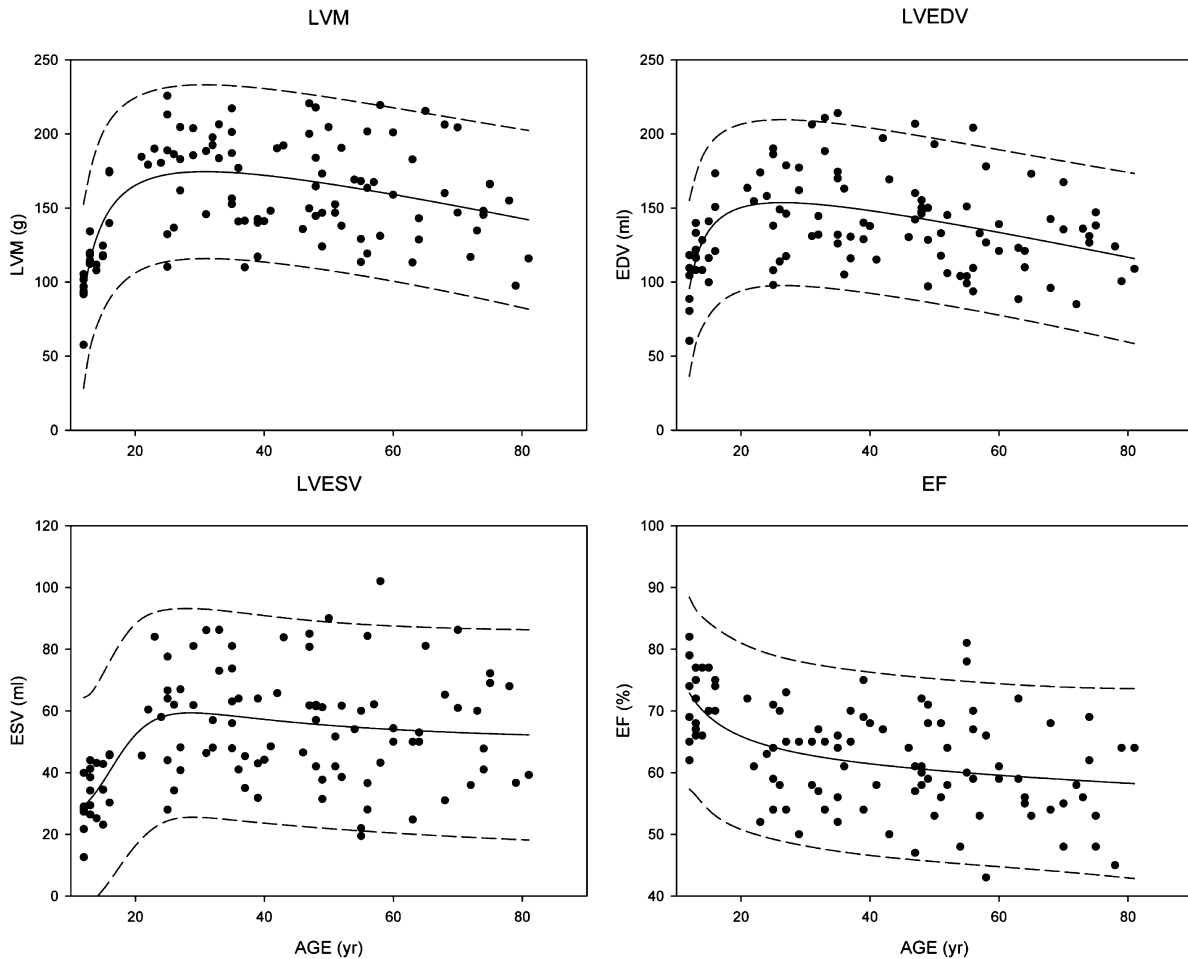


Figure 1.



Table 1. Normal values of LVM, EDV, ESV, and EF according to age and gender.

Age	10–19	20–29	30–39	40–49	50–59	60–69	>70	p
LVM (g) MALE	128±10	196±5	191±4	193±8	168±7	185±10	165±12	0.001
LVM (g) FEMALE	109±6	159±12	143±9	145±7	133±7	123±9	121±9	0.001
ESV (ml) MALE	36±3	68±3	69±4	68±6	53±8	55±7	61±9	0.001
ESV (ml) FEMALE	32±3	43±2	46±4	51±4	38±5	39±7	47±6	0.001
EDV (ml) MALE	124±10	163±5	178±9	170±9	138±14	132±11	140±9	0.001
EDV (ml) FEMALE	120±7	136±14	131±8	135±4	109±4	104±7	113±10	0.001
EF (%) MALE	72±12	63±9	63±10	60±9	65±12	64±11	65±10	0.001
EF (%) FEMALE	70±10	62±9	63±8	61±10	62±9	60±9	60±11	0.001

Introduction: How left ventricular mass (LVM), dimensions (LVD), and ejection fraction (EF) evolve in adolescence and vary with adult age is unclear. Previously defined MRI normal ranges of LVM and LVD have been described in studies of limited size, age-range, or in pts with risk factors.

Purpose: We sought to prospectively examine the normal physiological trend of LVM, LVD, and EF in truly normal pts from early adolescence to late adulthood and define normal ranges of these parameters according to age and gender.

Methods: 102 pts (55 males, 12–81 yrs) prospectively enrolled with normal ECG and without hypertension (<140/80) underwent cardiac MRI. Short axis turbo gradient images (TR 100 ms, TE 4.8 ms, ST 10 mm) were analyzed by experienced readers (Simpsons rule, manual delineation). LVM, end-diastolic volume (EDV), end-systolic volume (ESV), and EF were analyzed according to gender, adolescence (20 pts) vs. adulthood, and by 7 age groupings (ANOVA).

Results: LVM, EDV, and ESV rose rapidly during teenage years and slowly declined over the adult age-range ($p < 0.001$ all) (Figure 1). Gender differences were present for LVM in every age group (males higher LVM ($p < 0.001$)) and in most age groups for EDV and ESV (Table 1). EF declined during adolescence in both genders with little change thereafter. Adolescents displayed lower LVM (116±26 vs. 165±32 g, $p < 0.001$), EDV (116±24 vs. 141±31 ml, $p < 0.001$), ESV (33±13 vs. 56±18 ml, $p < 0.001$), but higher EF (72±5 vs. 60±7%, $p < 0.001$) compared to adults (Figure 1).

Conclusions: Normal LVM and LVD measured by MRI show a rapid physiological rise during adolescence and slow fall during adulthood. EF declines in from adolescence to adulthood in both men and women. Clear gender differences exist for LVM, EDV and less so for ESV. These findings may allow normal ranges of LVM and LVD to be developed from early adolescence to late adulthood.

324. LV Mass Index and the Common, Functional, X-linked Angiotensin II Type 2-receptor Gene Polymorphism (1332 G/A) in Patients with Systemic Hypertension

Khaled Alfakih,¹ Azhar Maqbool, PhD,² Gavin Bainbridge,¹ John Ridgway,¹ Anthony Balmforth,² Alistair Hall,³ Mohan Sivananthan.¹ ¹Cardiac MRI, Leeds General Infirmary, Leeds, United Kingdom, ²Institute of Cardiovascular Research, University of Leeds, Leeds, United Kingdom, ³Academic Unit of Cardiovascular Medicine, Leeds General Infirmary, Leeds, United Kingdom.

Introduction: A common intronic polymorphism, (–1332 G/A) of the angiotensin type 2 (T₂) receptor gene, located on the X-chromosome, has been reported to be biochemically functional.

Purpose: To evaluate the AT₂ receptor gene polymorphism (–1332 G/A) for an association with left ventricular hypertrophy (LVH).

Methods: LV mass was measured in 197 patients with systemic hypertension and 60 normal volunteers, using a 1.5-Tesla Philips MRI system. Genotyping was performed using a restriction enzyme digestion of an initial 310 bp PCR product that included the AT₂ (–1332 G/A) locus.

Results: The mean LV mass index for the male patients was 94.3±19.6 g/m² (n=125) and for the female patients was 71.2±12.0g/m² (n=72). Seventy three (37.1%) of all patients had an elevated LV mass index, defined as the mean LV mass index for normal volunteers plus 2 S.D (males 77.8±9.1 g/m², n=30; females 61.5±7.5g/m², n=30). Comparison of LV mass index, of the A/AA genotype (mean LV mass index=82.4±21.1 g/m²; n=123) against that of the G/GG genotype (mean LV mass index=88.1±19.0 g/m²; n=89), as a continuous variable was significant by analysis of variance ($p=0.044$). Chi-square comparison between normotensive volunteers without LVH (NT

LVH-) and hypertensive patients with LVH (HT LVH+) recorded a difference in genotype frequency (A/AA vs. G/GG) that was significant ($p=0.023$) (Fig 1).

Conclusions: We observed an association between the AT₂ receptor (−1332 G) allele and the presence of LVH in hypertensive subjects.

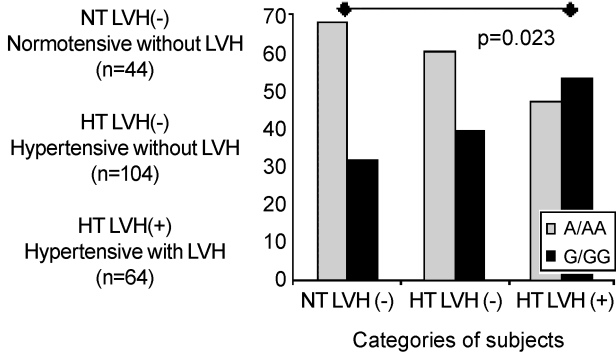


Figure 1.

325. Regression of Hypertrophy in Remote Myocardium After Percutaneous Transluminal Septal Myocardial Ablation in Hypertrophic Obstructive Cardiomyopathy: A MRI Follow-Up Study

Willem G. van Dockum,¹ Marco J.W Gotte, MD PhD,¹ Aernout M. Beek,¹ Folkert J. ten Cate, MD PhD,² Jurrien M. ten Berg, MD PhD,³ Mark B.M Hofman, PhD,¹ Cees A. Visser, MD PhD,¹ Albert C. van Rossum, MD PhD.¹ ¹Cardiology, VU University Medical Center, Amsterdam, Netherlands, ²Cardiology, Thoraxcenter Erasmus Medical Center, Rotterdam, Netherlands, ³Cardiology, St Antonius Hospital, Nieuwegein, Netherlands.

Introduction: Percutaneous transluminal septal myocardial ablation (PTSMA) in symptomatic patients with hypertrophic obstructive cardiomyopathy reduces the left ventricular (LV) outflow tract obstruction and decreases LV wall stress.

Purpose: The purpose of this study was to evaluate the early effects of PTSMA on regional myocardial thickness and regional myocardial mass with MRI.

Methods: In twenty-seven patients (age 52 ± 15 years) MR imaging was performed at baseline and at one and six-month's follow-up after PTSMA. With contrast-enhanced (CE-)MRI infarct size and location were determined. Changes in regional wall thickness,

LV volumes and regional myocardial mass were evaluated using cine imaging.

Results: After PTSMA, no infarction-related hyperenhancement was found outside the target area using CE-MRI. In patients with a successful gradient reduction ($n=24$), end-diastolic septal thickness at the infarct site decreased from 2.0 ± 0.4 cm at baseline to 1.3 ± 0.2 cm and 0.9 ± 0.3 cm at 1 and 6 month's follow-up, respectively ($p < 0.001$). Also the anterior, lateral and inferior wall thickness decreased significantly at both 1 and 6 month's ($p < 0.05$ and $p < 0.001$, resp.). As LV end-diastolic volumes remained unchanged, and LV end-systolic volumes increased ($p < 0.001$), ejection fraction decreased from $69 \pm 5\%$ to $65 \pm 5\%$ at 6 month's ($p < 0.001$). Total LV myocardial mass decreased from 207 ± 52 to 190 ± 49 g (-8%) and 165 ± 42 (-20%) at 1 and 6 month's, respectively ($p < 0.001$). Septal mass decreased from 73 ± 22 g to 64 ± 19 g (-12%) at 1 month and to 57 ± 17 g (-22%) at 6 month's ($p < 0.001$). The reduction of remote mass was significant at both 1 and 6 month's follow-up ($p < 0.001$), indicating early LV remodeling.

Conclusions: Septal ablation therapy in HOCM results in early LV remodeling with increased end-systolic volumes, normalization of EF, and regression of the remote myocardial hypertrophy.

326. MR Short Axis Ellipticity Index: A Reliable Indicator of Constrictive Pericardial Disease

F. Scott Pereles, MD,¹ Jeremy D. Collins, BS,¹ Gina K. Song, MD,¹ Amar Singh, MD,¹ James C. Carr, MD,¹ Tom Holly, MD,² Elizabeth Krupinski, PhD.³ ¹Radiology, Feinberg School of Medicine, Northwestern University, Chicago, IL, USA, ²Cardiology, Feinberg School of Medicine, Northwestern University, Chicago, IL, USA, ³Radiology, University of Arizona, Tucson, AZ, USA.

Introduction: Historically, echocardiography has been used as a first-line imaging modality to diagnose constrictive physiology in patients with pericarditis. This examination has relied primarily on changes in right ventricular configuration and filling, which are both insensitive and occur relatively late in the disease course, often in near tamponade states. Using balanced gradient echo cine MR imaging we have observed a change from the normal circular configuration of the left ventricle to an abnormal ovoid shape on short-axis images, as measured by a novel ellipticity index.



Purpose: The purpose of this study is to evaluate the reliability of a newly discovered cardiac magnetic resonance sign of constrictive pericardial disease called the ellipsicity index.

Methods: One hundred eighty-three consecutive cardiac MR examinations performed on a 1.5 T Siemens Sonata MR scanner were analyzed for the presence of an ovoid configuration of the left ventricle on cardiac short axis images. On these short axis images, the ellipsicity index was defined as the vertical height of the left ventricle divided by the horizontal mid chamber width at end diastole on a slice positioned equidistant between the mitral valve and the apex. All measurements were independently performed by two blinded physicians using electronic calipers on balanced gradient echo cine images displayed on General Electric PACS workstations. Of the 183 examinations, 26 cases were referred as clinically suspected cases of constrictive physiology on the basis of other imaging modalities and interventions: cardiac catheterization (5), echocardiography (12), serial follow-up examination (7), pericardiocentesis (1), pericardiectomy (4), pericardial biopsy (1) or pericardiectomy (1).

Results: ANOVA analysis indicated that the mean ellipsicity index for patients with proven constrictive physiology (1.36) was significantly higher than that those with either other cardiac pathology (1.23, $p=0.001$, degrees of freedom=1, 122, $F=10.89$) or normal cardiac examinations (1.25, $p=0.005$, degrees of freedom=1, 83, $F=8.50$).

Conclusion: The end-diastolic ovoid configuration of the left ventricle as measured by the ellipsicity index is a valuable addition to other MR findings as an indicator of constrictive physiology. Using our approach, an ellipsicity index of 1.30 appears to be a useful threshold to suggest the presence of constrictive physiology in the appropriate clinical setting.

327. The Incidence of Myocardial Scarring as Defined by Late Hyperenhancement in Patients with Acute Myocarditis

Jeanette Schulz-Menger, Hassan Abdel-Aty, Andreas Kumar, Rainer Dietz, Matthias G. Friedrich. *Cardiology, Franz-Volhard-Klinik, Charité, Berlin, Germany.*

Introduction: Contrast-enhanced CMR is able to detect inflammation as well as scarred tissue. In patients with acute myocarditis, we assessed the incidence of signal intensity changes 10 minutes after the contrast

bolus (“delayed hyperenhancement”) as a marker for necrosis or fibrosis and compared it to that of signal intensity changes during early steady state (“relative enhancement”).

Purpose: To investigate the incidence of inflammation and necrosis in patients with acute myocarditis.

Methods: We investigated 18 (14 men, 4 female; age: 38 ± 18 years) patients with clinically proven acute myocarditis as defined by a combination of the following:

- a history of viral infection within the last 2 weeks
- no evidence for coronary artery disease
- ECG abnormalities and/or significant increase of serologic markers for myocardial injury

Patients were studied 5 ± 1 days after the onset of symptoms in a 1.5 T cardiac scanner. To assess inflammation, we quantified signal intensity changes in axial multi-slice T1-weighted spin echo images before and after 0.1 mmol/kg Gd-DTPA (“relative enhancement”, RE). Myocardial scars were visualized by a multi-slice inversion recovery gradient echo sequence of the whole left ventricle (TI 200–250 ms; TR 5.5ms; TE 1.4ms, 10 mm slices, no spacing, individual TI to null myocardium), starting 10 minutes after additional 0.1 mmol/kg Gd-DTPA (“delayed hyperenhancement”, DE). In 14 patients, we assessed the Gd-DTPA washout over 15 min after the bolus. Global function and regional wall motion abnormalities (RWMA) were analyzed based on SSFP-derived images. Two blinded observers performed the analysis.

Results: In all patients the relative enhancement was increased (mean 7.9 ± 1.0 ; normal values < 4 ; $p < 0.05$). Ejection fraction was slightly decreased (mean $52.4\pm 3.3\%$), with 65% of all patients having normal values ($62.9\pm 1.1\%$). RWMA were observed in 11 patients (55%). A focal DE was visible in the subepicardial and middle myocardial layers of 8 patients (44%), all of them with RWMA. The group with RWMA showed a trend towards a lower EF, which was not significant (49.3% vs. 61.7%, $p=ns$). RE was significant higher in the RWMA group (10.6 ± 4.3 vs. 6.0 ± 2.0 , $p < 0.05$). In patients without late DE, inversion recovery sequences revealed significant regional hyperenhancement in 50% of the patients at minute 3 (signal intensity compared to remote 29 ± 9 vs. 23 ± 6 , $p < 0.05$), but there was no focal enhancement in later than minute 11 (signal 14 ± 7 compared to remote 9 ± 3 , $p < 0.05$).

Discussion: Contrast-enhanced CMR detects inflammation in patients even with a normal LVEF, but

only 44% of patients show regional hyperenhancement, which turns out to be focally present in subepicardial and middle, but not in subendocardial layers. Enhancement during the early steady state (RE) is useful to detect inflammation, but signal enhancement does not persist over a longer period. This is consistent with inflammation but not necrosis/fibrosis. These findings match autoptic studies, showing a low incidence of myocardial necrosis in acute myocarditis with a local distribution different to myocardial infarction. Thus, CMR may be a specific tool to differentiate acute inflammation from necrosis and both from ischemic injury. Further studies are warranted.

Conclusions: The incidence of necrosis is rather low resulting in a limited sensitivity of delayed enhancement imaging to diagnose acute myocarditis. The relative enhancement as assessed over a period of several minutes early after the bolus shows a higher sensitivity. The pattern of necrosis, if present, differs from that of ischemic necrosis and is likely to enable a specific differentiation from acute myocardial infarction in such a setting.

328. Assessment of Left Atrial Volume by Contrast Enhanced Magnetic Resonance Angiography-Comparison with Cine MR

Thomas H. Hauser, Seth McClennen, MD, Mark E. Josephson, MD, Warren J. Manning, MD, Susan B. Yeon, MD, JD. *Medicine, Cardiology Division, Beth Israel Deaconess Medical Center, Boston, MA, USA.*

Introduction: An increase in left atrial (LA) volume is associated with cardiovascular morbidity, particularly atrial fibrillation. Contrast-enhanced magnetic resonance angiography (MRA) visualizes the LA but the validity of LA volume measurements using this technique has not been evaluated.

Purpose: We compared LA volume measurements from MRA with cine magnetic resonance (MR) LA volume measurements.

Methods: We performed MRA and cine MR in 17 consecutive patients referred for MRA prior to atrial fibrillation ablation. LA volumes were calculated by disk summation in the axial (MRA) or 4-chamber (cine MR) imaging plane. MRA LA volumes were compared to cine MR LA volumes at the maximal LA size and at LA end-diastole using linear regression and limits of agreement analysis.

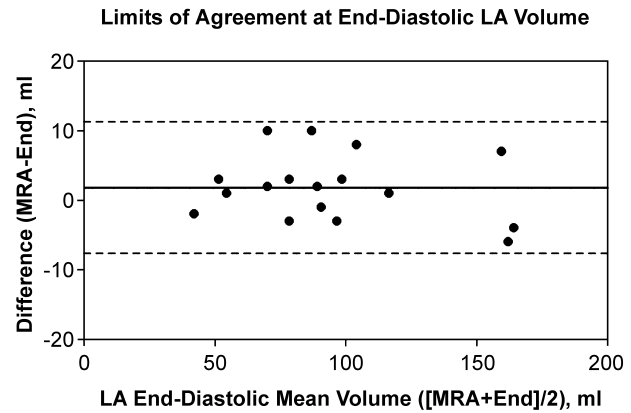


Figure 1.

Results: The cohort included 12 (71%) men and 5 (29%) women, age 48 ± 9 years. All subjects were in sinus rhythm at the time of imaging. The mean cine MR LA volume was 121 ± 38 ml at maximal LA size and 94 ± 38 ml at LA end-diastole ($p < 0.001$). LA volume determined by MRA was 96 ± 37 ml. The cine MR LA end-diastolic and MRA LA volumes were closely correlated ($R^2 = 0.98$, $p < 0.001$) with narrow 95% limits of agreement (-8 ml to 11 ml) (Figure 1). Although the MRA LA volume had a strong correlation with the maximal cine MR LA volume ($R^2 = 0.84$, $p < 0.001$), the 95% limits of agreement were relatively wide (-55 ml to 4 ml) (Fig. 1).

Conclusion: MRA LA volumes correspond most closely to LA end-diastolic cine MR LA volumes and are significantly smaller than the maximal LA volume. The relationship of MRA LA volume to cardiovascular morbidity remains to be defined.

329. The Accuracy and Reproducibility of Left Ventricular Volume and Mass Measurements Using a Dual Inversion Recovery Black Blood Sequence

Sarah R. Clay, BSc, Khaled Alfakih, MBBS, Timothy R. Jones, MSc, Gavin J. Bainbridge, DCR, John P. Ridgway, PhD, Mohan U. Sivananthan, PhD. *BHF Cardiac MRI Unit, Leeds General Infirmary, Leeds, United Kingdom.*

Introduction: Steady state free precession (SSFP) is now regarded as the 'gold standard' image acquisition method as it provides better definition between blood and muscle than conventional gradient echo. The



Table 1. The observer variability expressed as the standard deviation of the difference between two values.

	LV EDV interobserver variability	LV EDV intraobserver variability	Mass interobserver variability	Mass intraobserver variability
SSFP SDD(SDD%)	5.7 (3.3%)	4.7 (5.2%)	4.5 (3.7%)	2.9 (4.7%)
BB SDD (SDD%)	8.6 (5.4%)	10.0 (6.3%)	3.3 (2.3%)	3.6 (5.0%)

SDD=standard deviation of difference between two values, SDD%=SDD expressed as a percentage of the mean result.

improvements in endocardial border definition seen with SSFP are however not observed at the epicardial border, which is often difficult to define accurately. Preliminary observations into the use of black blood (BB) cardiac magnetic resonance (CMR) pulse sequences showed improved epicardial border definition as well as good endocardial border definition, because of complete suppression of the blood signal.

Purpose: The aim of this study was to compare left ventricular (LV) mass and LV end-diastolic volume (EDV) measurements and the observer variability between images acquired with a dual inversion recovery BB sequence and SSFP.

Methods: Images were acquired from 16 healthy volunteers, 2 patients with left ventricular hypertrophy and 2 patients with dilated ventricles using SSFP and black blood sequences in the short-axis orientation. The sequence parameters are summarised below:

- a) BB; TR=1 × RR, TE=39 msec, flip angle=90 degrees, acquisition matrix=384 × 512, FOV=290, 6-mm slice thickness, 4-mm interslice gap, 1 phase/cardiac cycle, 2 slices per 10–12 second breath hold.
- b) SSFP; TR=3.34 msec, TE=1.67 msec, flip angle=55 degrees, bandwidth=1042 Hz/pixel, acquisition matrix=192 × 163, FOV=360 ×

288 mm, half Fourier acquisition matrix 6-mm slice thickness, 4-mm interslice gap, 18 phases/cardiac cycle, with two slices acquired per 10- to 12-second breath hold.)

MASS software was used to analyse the images and the LV EDV and LV mass were calculated by a modified Simpson’s rule.

Results: The mean±one standard deviation for LV EDV was 178.3±52.7 ml measured with SSFP and 158.8±62.2 ml with BB. This difference was not statistically significant (p=0.22). For SSFP the mean value of LV mass was 124.0±27.0 g and 147.5±37.4 g for BB, a statistically significant difference (p<0.0001). Examining the observer variability (Table 1) showed BB imaging to be at least as reproducible as SSFP for LV mass which may be a result of better epicardial definition with a BB technique. The non-significant paired t test result for the difference in EDV measurements may be a result of a variable trigger delay set at the end of the R–R interval in the dual inversion recovery BB sequence. This may have lead to the ED images being acquired before the ventricle had fully dilated in some patients (Figure 1).

Conclusions: The dual inversion recovery BB imaging showed that with further evaluation it could be as good as SSFP for accuracy and reproducibility of LV mass measurements. A separate normal range would need to be established.

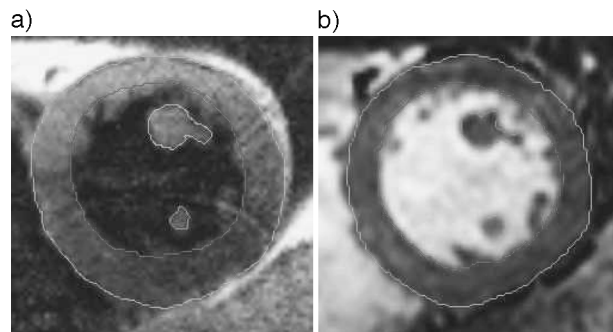


Figure 1. a) A BB short-axis image with endocardial and epicardial contours in place on the LV. b) A SSFP short-axis image with epicardial and endocardial contours in place on the LV. (View this art in color at www.dekker.com.)

330. Measurement of Aortic Root Size by Cardiovascular Magnetic Resonance

Elisabeth D. Burman, MSc, Dudley J. Pennell, MD FRCR FESC FACC, Philip J. Kilner, MD PhD. *Cardiovascular Magnetic Resonance, Royal Brompton Hospital, London, United Kingdom.*

Introduction: Accurate and reproducible measurements of aortic root dimensions are crucial for informed decision making on the timing and nature of surgical replacement of the aortic valve or root. Values for normal

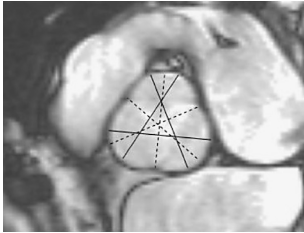


Figure 1.

aortic root dimensions have previously been determined by echocardiography using methods that differ from those available to cardiovascular magnetic resonance (CMR). CMR is now widely available and gives virtually unrestricted access to the aorta in any chosen plane, but methods of acquisition and measurement, and corresponding normal ranges have still to be determined.

Purpose: To measure aortic root dimensions by CMR using specified planes of acquisition and defined dimensions, and to establish normal ranges with respect to gender and age.

Methods: Sixty healthy normotensive volunteers were selected (31M, 29F, age range 20–79). They comprised three groups aged 20–40, 40–60 and 60–80 years, with ten subjects of each gender in each age range. CMR was performed using a 1.5 T Siemens Sonata scanner. Two orthogonal TrueFISP cines aligned with the left ventricular outflow tract (oblique sagittal and oblique coronal) were acquired from transaxial and coronal multislice scouts. From these in-plane cines, two planes transecting the aortic root at its point of maximum diameter, mid aortic sinus level, were acquired at mid systole (at the time of maximum distension) as illustrated in the Figure 1, and at end diastole. From each of

these cines, 6 aortic root dimensions were measured. Measurements were made from each of the three cusps to the opposite commissure (cusp to commissure-dotted lines in Figure 1) and from each cusp to the furthest point on the adjacent cusp (cusp to cusp-continuous lines). Due to the movement of the root during the cardiac cycle, systolic measurements were taken from the acquisition aligned at mid-systole, and diastolic measurements from the acquisition aligned at end diastole. The average of each set of 3 measurements was taken.

Results: The means ± standard deviations (and 95% confidence intervals) for respective groups are shown in the Tables 1 and 2. Aortic root dimensions were typically found to be larger by 5 mm in males than in females. Comparing the 20–40 year olds with the 60–80 year olds, dimensions increased by 3 to 4 mm over 40 years. Maximum cusp to cusp dimensions were larger than cusp to commissure measurements by about 2 mm. Dimensions were larger in systole than in diastole by only about 1 mm.

Conclusions: We report normal aortic root dimensions measured by CMR which show the importance of gender and age differences. The location and timing of measurements should be defined for reproducibility of results.

331. Integrated Approach to the Evaluation of the Hypertensive Patient Using Cardiac MRI

Alicia M. Maceira, MD, Sanjay K. Prasad, MD, Raad Mohiaddin. *CMR Unit, Royal Brompton Hospital, London, United Kingdom.*

Table 1. Aortic root dimensions from cusp to commissure in mm.

Age (years)	Male systolic	Female systolic	Male diastolic	Female diastolic
20–40	32 ± 3.4 (25–38)	27 ± 2.4 (23–32)	30 ± 3.4 (23–36)	25 ± 2.3 (21–29)
40–60	33 ± 4.1 (25–40)	29 ± 2.0 (25–32)	31 ± 4.1 (24–39)	27 ± 2.0 (24–31)
60–80	35 ± 2.5 (30–39)	30 ± 1.4 (27–32)	34 ± 2.1 (30–38)	28 ± 1.7 (25–32)
All subjects	33 ± 3.5 (26–40)	28 ± 2.2 (24–33)	32 ± 3.6 (25–38)	27 ± 2.4 (22–31)

Table 2. Aortic root dimensions from cusp to cusp in mm.

Age (years)	Male systolic	Female systolic	Male diastolic	Female diastolic
20–40	33 ± 4.1 (26–41)	28 ± 3.0 (23–34)	32 ± 3.7 (25–39)	27 ± 3.0 (21–32)
40–60	35 ± 5.0 (25–45)	31 ± 2.7 (26–36)	34 ± 5.3 (24–44)	30 ± 2.2 (25–34)
60–80	37 ± 3.0 (31–43)	32 ± 1.9 (28–35)	36 ± 2.9 (31–42)	31 ± 2.3 (26–35)
All subjects	35 ± 4.3 (27–43)	30 ± 2.8 (25–36)	34 ± 4.4 (26–42)	29 ± 2.9 (23–34)



Introduction: Long standing hypertension (HTN) causes significant cardiac morbidity. Accurate evaluation is important to exclude potential remediable secondary causes. Several diagnostic imaging tests are usually required both to rule out some of the commonest causes of secondary HTN and to measure left ventricular mass and function. Cardiac Magnetic Resonance (CMR) can provide an integrated approach to the hypertensive patient, producing a fast diagnosis and making other tests unnecessary.

Purpose: To assess the feasibility of CMR and magnetic resonance angiography (MRA) to accurately define cardiac mass and volume and exclude some of the commonest causes of secondary HTN including aortic coarctation, renal artery stenosis and adrenal gland pathology.

Methods: Forty-eight patients with HTN referred for CMR study between October'02 and April'03 were included. The reasons for referral were early-onset HTN (n=18), HTN resistant to drug therapy (n=20), paradoxical response to BB therapy (n=1), and increase in creatinine with ACEi (n=10). The CMR studies were performed on a Siemens Sonata 1.5 T scanner. The study protocol included: 1) a multislice dark blood (HASTE) sequence in transverse orientation of the thorax to provide an overview of the cardiovascular anatomy, 2) TrueFISP cine VLA, four-chamber and short-axis images to measure left ventricular mass and function plus an aortic arch cine to exclude coarctation, 3) HASTE multislice and T2 weighted turbospin-echo slices (7 mm slice thickness, 3 mm gap) in transverse and coronal views of the upper abdomen to scan the adrenal glands and measure renal dimensions and 4) 3D contrast-enhanced MRA of the renal arteries with Gadolinium-DTPA (0.2 mmol/Kg). The average scanning time for the whole protocol was 45 minutes.

Results: Significant abnormalities were found in 12 patients (25%): adrenal mass (n=1), aortic coarctation (n=3) and significant renal artery stenosis (n=8); three left renal artery stenoses, three right renal artery stenoses and one bilateral stenosis more severe on the right), one of these subjects also had significant hydro-nephrosis and another two intrinsic renal disease. Mean LV mass index was 136 ± 32 gr/m², which was increased when compared to normal reference values, LVEF was preserved ($64 \pm 10\%$), no wall motion abnormalities were detected.

Conclusions: CMR/MRA can provide a comprehensive evaluation of patients with HTN and allows for a unique integrated approach with assessment of LV mass, function and wall motion abnormalities as well as in the detection of secondary causes.

332. Right Ventricular Intramyocardial Fatty Infiltration is Associated with Diastolic Dysfunction

Raymond Q. Migrino, MD,¹ Suhny Abbara, MD,² Ricardo Cury, MD,² David Sosnovik, MD,¹ Thomas Brady, MD,² Godtfred Holmvang, MD.¹ ¹Radiology and Medicine, Massachusetts General Hospital, Boston, MA, USA, ²Radiology, Massachusetts General Hospital, Boston, MA, USA.

Introduction: Intramyocardial fatty infiltration (IMF) is a major criterion for the diagnosis of arrhythmogenic right ventricular dysplasia (ARVD) and has arrhythmogenic potential. The functional significance of right ventricular (RV) IMF in the setting of preserved systolic function is not known.

Purpose: The study aims to determine whether IMF is associated with impaired RV diastolic function.

Methods: Twenty four patients underwent cardiac magnetic resonance imaging between 2002 and 2003 for ARVD assessment. Cine acquisition of RV function was performed (field of view 14–16 cm, slice thickness 5.5–7 mm, temporal resolution 23–54 ms) on contiguous slices in the axial view. The RV endocardial contour was traced, volume was calculated using the Simpson's method and volume–time curve throughout the cardiac cycle was obtained. All patients had normal RV systolic function and were divided into 2 groups: I: no IMF and II: IMF present (+). Indices of diastolic filling were compared between the groups: peak filling rate (PFR) (peak instantaneous change in volume over change in time), time to peak filling rate (TPFR), filling fraction at 200 ms (FF200) (change in volume in first 200 ms of diastole over stroke volume).

Results: (see Table 1).

Conclusions: The presence of RV IMF is associated with diminished peak filling rate and early diastolic filling fraction. IMF in the RV is associated with impaired diastolic function and may be an early manifestation of functional impairment preceding systolic dysfunction.

Table 1.

	No IMF (n=9)	IMF (+) (n=15)	p value
Cycle length (ms)	748±100	859±38	0.24
RVEF (%)	60±2	55±2	0.11
PFR (mL/ms)	3.1±0.4	2.3±0.2	0.04
TPFR (ms)	72±10	105±13	0.08
FF200 (%)	66±3	47±4	0.001

333. Lesion Patterns in Patients After Septal Ablation in Hypertrophic Cardiomyopathy—Relation to the Interventional Approach

Jeanette Schulz-Menger,¹ Hassan Abdel-Aty,¹ Hartmut Goos,² Rainer Dietz,¹ Matthias G. Friedrich.¹
¹Cardiology, Franz-Volhard-Klinik, Charité, Berlin, Germany, ²Cardiology, Klinikum Uckermark, Schwedt, Germany.

Introduction: Septal ablation is an accepted option in patients with hypertrophic obstructive cardiomyopathy. The usual approach uses intracoronary alcohol application to induce myocardial infarction. This technique however is hampered by the occurrence of persistent AV-bundle branch-block, presumably due to the extensive tissue destruction. Another approach uses microparticles to embolize the artery with a low rate of reported AV blocks. Although the size and type of lesion likely determines the complication rate, there are no comparative reports on lesion morphology in the different approaches. Contrast-enhanced CMR can be used to characterize the septal lesions.

Purpose: Lesion morphology and extent as detected by contrast-enhanced CMR differ in patients with embolic septal infarction as compared to alcohol-induced necrosis.

Methods: We investigated 7 (6 men age: 50±12 years) patients 3,6±2 years after alcohol ablation and 20(15 men age: 60±4 years) patients (A) 3,7±2 years after microparticle (M)administration. The amount of alcohol was 2 ml in each patient, that of polyvinyl alcohol foam particles 5.2±0.8 ml. A multi-slice inversion recovery gradient echo sequence was applied in 1.5 T MRI systems to visualize myocardial scarring (hyperenhancement) (TR 5.5 ms; TE 1.4 ms, slice thickness 10 mm, no spacing, individual TI) 10 minutes after the second bolus of Gd-DTPA. Function and mass were quantified in SSFP images.



Figure 1.



Figure 2.

Results: In both groups the ejection fraction was normal (A:75.1±3 vs. M:76.8±3%, p=n.s.), the left ventricle showed a hypertrophy (A:232.9±16 vs. M:277.0±27). There were no significant differences between the groups. In all patients the induced infarcts were detectable and the scan duration was 30–45 minutes. In the alcohol group (Figure 1) the infarcted area was significantly larger than in the emboli group (Figure 2) (A:11.1±2.6 g vs. M:7.4±0.7 g; p<0.05) and more likely to be transmural (5/7 vs. 2/20). The improvement of clinical outcome was the same in both groups (NYHA 3before/NYHA I after.)

Discussion: The advantages of contrast enhanced CMR should be used in systematic studies on the relation of lesion patterns to complications and thus guide interventional approaches.

Conclusions: The advantages of contrast enhanced CMR should be used in systematic studies on the relation of lesion patterns to complications and thus guide interventional approaches.

334. Septal Fibrosis and Skeletal Muscle Abnormalities in Familial Cardiomyopathy

Subha V. Raman, MD, MS, Elizabeth A. Sparks, RN, Matthew Neff, BA, Steven D. Nelson, MD, Charles F. Wooley, MD. *Internal Medicine, Ohio State University, Columbus, OH, USA.*

Introduction: Over the past 5 decades, our institution has had the opportunity to investigate a large kindred with a frameshift mutation in the lamin A/C gene resulting in cardiac conduction abnormalities and progressive cardiomyopathy. Autopsy studies have demonstrated fibrosis in the mid ventricular septum; antemortem non-invasive identification would be useful for risk stratification of genotype-positive members of the kindred.



Purpose: We sought to test the utility of magnetic resonance examination with delayed myocardial enhancement (DME) acquisition for noninvasively identifying midseptal fibrosis and other changes in a group of early affected genotype-positive family members as well as age- and sex-matched controls.

Methods: Subjects provided written informed consent to participate in an Institutional Review Board-approved study. CMR examination with gadolinium-DTPA administered through a peripheral intravenous line included comprehensive assessment of atrial and ventricular size and function, DME acquisitions, as well as a novel calf muscle imaging protocol. Images from all subjects were reviewed offline in random order.

Results: No significant difference was observed in atrial volumes or ventricular size or function between early affected family members and controls. Subtle changes on DME imaging were observed in the mid-ventricular septum in 3 of 13 Family members and in 0 of 18 controls. Striking changes in the calf muscles with conventional spin echo, spin echo with fat saturation, and DME applied to the calf were noted in 3 of 13 Family members (see images below) whereas none of the controls demonstrated these skeletal muscle abnormalities (Fig. 1).

Conclusions: A comprehensive CMR examination including lower extremity assessment may be useful in detection of myocardial fibrosis as well as skeletal muscle involvement in a family with hereditary cardiomyopathy.

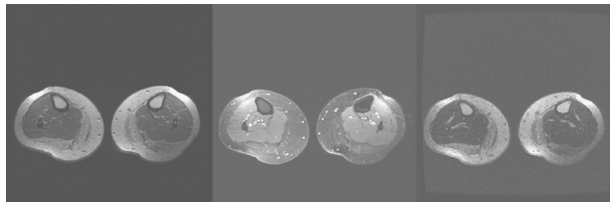


Figure 1.

335. Fat Detection with Dual Inversion-Recovery Fast Spin-Echo MRI in Arrhythmogenic Right Ventricular Dysplasia/Cardiomyopathy (ARVD): A Cadaver and Patient Study

Ernesto Castillo Gallo, MD,¹ Harikrishna Tandri, MD,² E Rene Rodriguez, MD,³ Khurram Nasir, MD,² Julie Rutberg, MS,² Hugh Calkins, MD,² Joao A. C. Lima, MD,² David A. Bluemke, MD.¹ ¹Radiology, Johns

Hopkins University, Baltimore, MD, USA, ²Cardiology, Johns Hopkins University, Baltimore, MD, USA, ³Pathology, Johns Hopkins University, Baltimore, MD, USA.

Introduction: Fibrofatty infiltration of the right ventricle (RV) is the histopathologic hallmark of arrhythmogenic right ventricular dysplasia/cardiomyopathy (ARVD/C). Dual inversion-recovery fast spin-echo (DIR-FSE) overcomes the limitations of long scan times and insufficient blood suppression of the ECG-gated spin-echo (SE) sequence.

Purpose: To assess the use of MR imaging in depicting intramyocardial fat with DIR-FSE compared to gated-SE in cadaveric heart specimens, and patients with ARVD/C.

Methods: The limiting in-plane spatial resolution of gated-SE and DIR-FSE imaging protocols (including TR of 1 and 2 R-R intervals, and echo train length ranging 12–32) was determined with an American College of Radiology MR phantom. Two cadaveric specimens with proven ARVD of women aged 18–35 years (mean age: 26.5 years) were imaged using the same pulse sequences with the addition of spectrally selected fat suppression. Contrast-to-noise ratios (CNR) of the intramyocardial fat in the right ventricle were measured and compared using analysis of variance (ANOVA) and Student t-test with Bonferroni correction. Eleven patients (6 female, 5 male; mean age, 36.9 years; range, 16–58 years) and 10 control subjects (4 female, 6 male; mean age, 33 years; range, 25–41 years) underwent DIR-FSE imaging. Images were evaluated semiquantitatively in terms of fat conspicuity and image quality using rating scales of 1–4. Differences between patients with ARVD and the control group were also assessed by the Student t-test.

Results: The DIR-FSE sequences achieved better limiting spatial resolution but lower CNR than gated-SE. The measured absolute CNR in the cadaveric specimens was larger for DIR-FSE with spectrally selected fat suppression than without it ($P < .05$). Cadaveric specimens demonstrate fat infiltration from the epicardium toward the endocardium of the right ventricle free wall. Intramyocardial fat was detected in 8/11 (72.7%) of ARVD patients and in none of the normal volunteers ($P < .001$) using a 2R–R DIR-FSE sequence with a TE=30, 5 mm slice thickness, ETL of 24–32 or less, and FOV of 28 cm.

Conclusions: DIR-FSE MR pulse sequences combined with fat suppression techniques are more advantageous for intramyocardial fat detection in ARVD/C compared to gated-SE imaging. However, when DIR-FSE is applied in vivo, breathholding constraints limit the spatial resolution of MRI for fat detection within the right ventricle.



336. Morphologic and Functional Right Ventricular Abnormalities in Arrhythmogenic Cardiomyopathy

Yves Provost, MD, Tracy Elliot, MD, Narinder Paul, MD, Naeem Merchant, MD. *Radiology, UHN, Toronto, ON, Canada.*

Introduction: Intramyocardial fat infiltration is the histologic hallmark of the arrhythmogenic cardiomyopathy. It is commonly associated with focal or diffuse right ventricular dilatation, wall thinning or hypertrophy and wall motion abnormalities. The MR appearances of these abnormalities may be subtle and nonspecific, at times in the range of the normal.

Purpose: To review the MR appearances of right ventricular abnormalities in arrhythmogenic cardiomyopathy and identify more specific pattern of abnormality.

Methods: We have reviewed the cardiac MRI of the last 25 consecutive patients with a confirmed diagnosis of arrhythmogenic cardiomyopathy in our hospital. The right ventricular abnormalities were recorded and compared with the examinations of 50 other consecutive patients with initial clinical suspicion of arrhythmogenic cardiomyopathy and that subsequently did not meet the criteria of arrhythmogenic cardiomyopathy. All the patients underwent cardiac MRI using 1.5 T magnet and dedicated cardiac phased-array coil. Cine MRI using a FIESTA pulse sequence in axial and short axis oblique views plus axial spin-echo DIR sequence with and without fat saturation were performed.

Results: Most of the patients with confirmed arrhythmogenic cardiomyopathy showed a combination of multiple morphologic and functional abnormalities of the right ventricle rather than isolated findings. Focal and subtle findings tended to be nonspecific particularly when isolated.

Conclusions: The range of right ventricular abnormalities in arrhythmogenic cardiomyopathy is reviewed. The combination of multiple morphologic and functional abnormalities of the right ventricle, rather than isolated findings, is strongly associated with the diagnosis of arrhythmogenic cardiomyopathy.

337. Detection of Myocardial Fibrosis in Systemic Hypertension Using Delayed-Enhancement Magnetic Resonance Imaging

Alicia M. Maceira, MD, James C. C. Moon, Sanjay K. Prasad, MD, Raad Mohiaddin, MD. *CMR Unit, Royal Brompton Hospital, London, United Kingdom.*

Introduction: Left ventricular hypertrophy related to chronic primary systemic hypertension (HT) is associated with an exaggerated accumulation of collagen, particularly in the interventricular septum and free wall, resulting in increased myocardial stiffness. This is linked to abnormalities of cardiac function, electrical activity and intramyocardial perfusion. The presence of myocardial fibrosis has been noninvasively assessed by measurement of plasma peptides, but is difficult to study with imaging techniques. Delayed-enhancement Magnetic Resonance Imaging (DE-MRI) has been shown to be able to distinguish scarred myocardium (hyper-enhanced) from normal viable myocardium (dark) in pathologies such as ischaemic cardiomyopathy, hypertrophic cardiomyopathy, Fabry's disease, and other conditions.

Purpose: To detect for the presence of myocardial fibrosis by DE-MRI in hypertension and its correlation with parameters of cardiac dysfunction including ejection fraction and ventricular mass.

Methods: 35 consecutive HT patients studied (57±12 yrs, 24 male) between November'02 and April'03 were included. Mean duration of HT was 7±4 yrs. All subjects with previous history of (or symptoms/ECG changes suggestive of) ischemic heart disease were excluded. The studies were performed on a Siemens Sonata 1.5 T scanner. The study protocol included: 1) thoracic dark blood (HASTE) multislice sequence in transverse orientation for an overall view of cardiac anatomy, 2) TrueFISP cines of VLA, HLA, four -chamber as well as SA stack (7 mm slice thickness with 3 mm gap) to study cardiac anatomy and function and 3) a peripheral bolus injection of gadolinium-DTPA (0.2 mmol/kg) was given, and contrast-enhanced images were acquired using a segmented inversion-recovery sequence. Imaging commenced 20 min after Gd-DTPA was given; segmentation was from 17 to 23 lines; inversion pulse every 2 to 3 heart beats depending on the RR interval and heart rate variability; a 90° presaturation pulse was placed over the cerebrospinal fluid to eliminate ghosting; VLA, HLA, four chamber and all SA views were acquired in duplicate but with reversed phase-encoding direction and the inversion time was optimised for each scan to ensure myocardial nulling.

Results: Mean LVMI was 136±32 g/m². Global and regional systolic function were in the normal range. In 5 subjects (14%) there was myocardial late hyperenhancement (1 female, 4 male). In 1 case, hyperenhancement was located in the papillary muscles, and in the other 4 the distribution was always midwall and located in the interventricular septum (n=3) and lateral wall (n=1). In three cases in which coronary angiography was available there were no detectable coronary lesions. No significant differences



were found between patients with and without myocardial enhancement with respect to age, gender, ventricular mass, years of HT and therapy.

Conclusions: DE-MRI reveals myocardial hyper-enhancement in a proportion of patients with systemic hypertension, not related to coronary artery disease. The presence and extent of hyperenhancement does not seem to correlate with conventional indicators of cardiac dysfunction such as increased ventricular volumes and mass or reduced ejection fraction. Further work is being undertaken to determine the long-term significance of these findings.

338. Diastolic Function to Assess Myocardial Iron in Thalassemia Major

Mark A. Westwood,¹ Alicia M. Maceira, MD,¹ Beatrix Wonke,² John B. Porter, PhD,³ Malcolm J. Walker, MD,⁴ Dudley J. Pennell, MD.¹ ¹CMR Unit, Royal Brompton Hospital, London, United Kingdom, ²Department of Haematology, Whittington Hospital, London, United Kingdom, ³Department of Haematology, University College Hospital, London, United Kingdom, ⁴Department of Cardiology, University College Hospital, London, United Kingdom.

Introduction: Cardiac failure due to iron overload remains the commonest cause of death in patients with thalassemia major (TM) in developed countries, accounting for 71% of all deaths. Due to the lack of a sensitive diagnostic test for myocardial iron overload, diastolic dysfunction in TM has not been previously demonstrated. Diastolic dysfunction may precede systolic dysfunction in cardiomyopathy, and thus may be an early functional marker of iron loading. CMR T2* measurements allow accurate determination of myocardial iron levels. We therefore compared the diastolic function and myocardial iron burden of thalassemia major patients using CMR.

Purpose: To assess diastolic function in iron induced cardiomyopathy.

Methods: 67 patients with TM were studied, all of whom were regularly transfused. For the measurement of myocardial T2*, a single short axis mid-ventricular slice was acquired at eight echo times (2.6–16.74 ms, which increased in 2.02 ms increments) in a single breath-hold. A gradient-echo sequence was used with a flip angle of 35°, a matrix of 128 × 256 pixels, a field of view of 40 cm, and a sampling bandwidth of 810 Hz per pixel. The Repeat Time between the 8 radiofrequency pulses applied each cardiac cycle was 20 ms. A delay time of 0 ms after the R wave trigger was chosen in order to

obtain a high quality image when blood flow and myocardial wall motion artefacts are also minimal. A homogeneous full-thickness region of interest was chosen in the left ventricular septum, encompassing both epicardial and endocardial regions. The signal intensity of this region was measured for each image using in-house designed software (CMRtools, © Imperial College), and this was then plotted against the echo time to form an exponential decay curve of the form $y = Ke^{-TE/T2^*}$ where K represents a constant, TE represents the echo time and y represents the image signal intensity. Retrospectively gated TrueFISP sequential short axis cines (7 mm slice thickness, 3 mm gap) were acquired, (echo time 1.63 msec, repeat time 22.75 msec, flip angle 60°, matrix 256 × 162 pixels), with at least 45 phases per cardiac cycle (temporal resolution between phases of less than 25 ms). Using in-house software a left ventricular blood volume time curve can be constructed. From this the change in blood volume over time can be derived, giving 2 distinct diastolic filling peaks corresponding to the early peak filling rate (EPFR) due to left ventricular relaxation and the atrial peak filling rate (APFR) due to atrial systole respectively. The ratio between these can also be calculated. Ten age and sex matched controls were also scanned, to determine the normal ranges for these parameters.

Results: The normal ranges obtained were: EPFR 711 ± 236 ml/s, APFR 240 ± 62 ml/s and EPFR/APFR ratio 3.0 ± 0.8. Out of the 67 patients, 45 had significant myocardial iron loading (myocardial T2* < 20 ms). With the iron loaded patients, the T2* correlated with both APFR (r = 0.48, P = 0.001, Figure 1) and EPFR/APFR ratio (r = 0.62, P < 0.000, Figure 2), but not the EPFR. The means of these parameters were significantly different between controls and iron loaded patients (APFR 174 ± 240 ml/s, p = 0.01, EPFR/APFR ratio

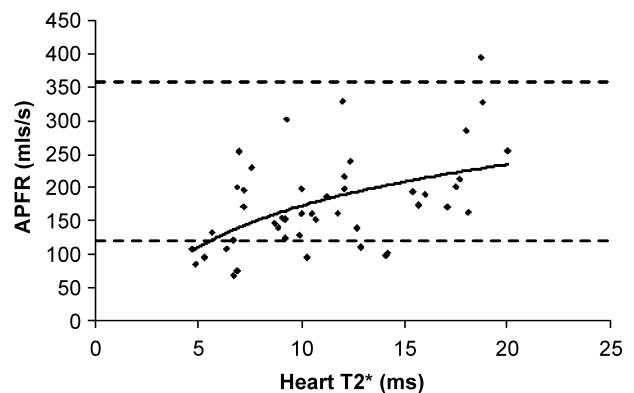


Figure 1. Relationship between APFR and the myocardial iron burden (myocardial T2*) with a logarithmic correlation curve shown. The upper and lower 95% confidence intervals are shown via the dotted lines.



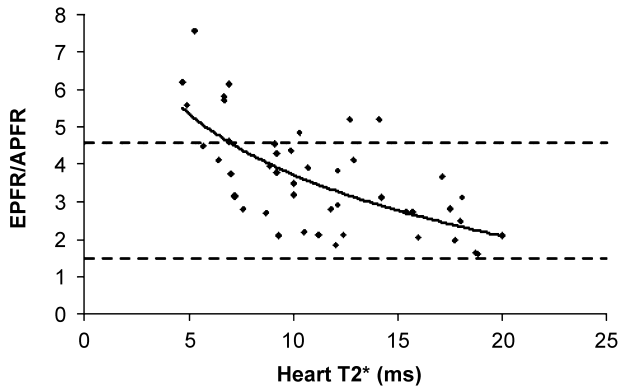


Figure 2. Relationship between EFPR/APFR ratio and the myocardial iron burden (myocardial T2*) with a logarithmic correlation curve shown. The upper and lower 95% confidence intervals are shown via the dotted lines.

3.7±1.4, p=0.009), but not between controls and non iron loaded patients.

Conclusions: Myocardial iron loading causes diastolic dysfunction, and myocardial iron loading may be a useful adjuvant in the assessment of myocardial iron loading. However, with the large overlap with the normal ranges may indicate the use of T2* CMR to assess early myocardial iron loading is more reliable.

339. Identification of Fibrotic Form of Arrhythmogenic Right Rentricular Dysplasia/ Cardiomyopathy Using Gadolinium-Enhanced Cardiovascular Magnetic Resonance

João L. F. Petriz, MD,¹ Marcelo Hadlich, MD,² Luis Antônio Mendonça, PhD,² Olga de Souza, MD,³ Lauro Pereira,² Clério Azevedo Filho, MD,² Gustavo Lacerda, MD,⁴ Francisco Manes Albanesi Fífho, MD,⁴ Jorge Moll Filho, MD,² Carlos E. Rochitte, MD.⁵ ¹Cardiovascular Magnetic Resonance, Rede D’Or & Labs and Rio de Janeiro State University, Rio de Janeiro, Brazil, ²Cardiovascular Magnetic Resonance, Rede D’Or & Labs, Rio de Janeiro, Brazil, ³Clinical Cardiology, Rede D’Or & Labs, Rio de Janeiro, Brazil, ⁴Clinical Cardiology, Rio de Janeiro State University–UERJ, Rio de Janeiro, Brazil, ⁵Cardiovascular Magnetic Resonance, Rede D’Or & Labs and Heart Institute–InCor–University of São Paulo Medical School, Rio de Janeiro, Brazil.

Introduction: Arrhythmogenic right ventricular (RV) dysplasia/cardiomyopathy (ARVD/C) is a heart muscle disease characterized by structural and functional abnormalities of the RV due to replacement of the

myocardium by fatty and fibrous tissue, leading to electrical instability that precipitates ventricular arrhythmias and sudden death. Replacement of the RV myocardium by fibrofatty tissue has been related to myocardial dystrophy and might reflect genetic abnormality, but inflammatory heart disease which patchy acute myocarditis with myocyte death was described in almost two thirds of cases and may involve both RV and Left Ventricle (LV). The diagnosis of ARVD/C is usually based on symptoms, right precordial EKG changes, RV arrhythmias, and structural and functional RV abnormalities. At the other extreme of the spectrum are patients in whom the diagnosis of ARVD/C was not recognized at onset of symptoms but who presented later with congestive heart failure with or without ventricular arrhythmias. Several cases have not been recognized because patients were asymptomatic until first presentation with malignant arrhythmias or sudden death and were difficult to diagnose by non-invasive methods. Gadolinium-enhanced cardiovascular magnetic resonance (CMR) can well characterize areas of myocardial fibrosis or necrosis and therefore might be useful to identify the fibrofatty form of ARVD/C.

Purpose: Demonstrate the usefulness of gadolinium-enhanced CMR as a clinical tool to identify the presence, extension and anatomical distribution of myocardial fibrosis in 2 patients with clinical diagnosis of ARVD/C.

Methods: The MR studies were performed using a 1.5 T Magnet (Siemens), with the following sequences: Anatomical: T2 Turbo Spin Eco. TR 1975, TE 57 ms, FOV 380 matrix 165×256, Slice Thickness/Gap 8.0/2.0, WFS 0.46 pixels. Myocardial delayed enhancement: patients received 0.4 mmol/kg of gadolinium-based contrast 10–20 minutes prior to image acquisition. Gradient-echo with an inversion-recovery preparation pulse using the following parameters: TR 2560, TE 3.4 ms, TI 140–160 ms, Flip Angle 25°, FOV 350, matrix 165×256, Slice Thickness/Gap 8.0/2.0, WFS 0.46 pixels.

Results: Patient (pt) 1 was a 38-year-old-male and pt 2 was a 28-year-old-female, both Caucasians. **Pt 1:** Patient presented palpitation and it was detected a episode of sustained atrial fibrillation. converted to sinus rhythm with amiodarone. Referred to a cardiologist, who did not find abnormalities at the physical

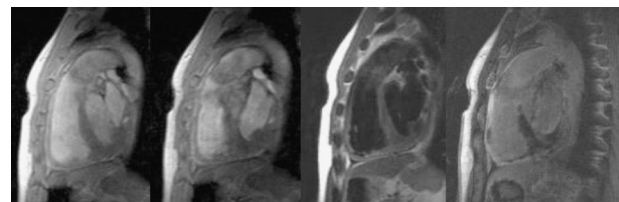


Figure 1.



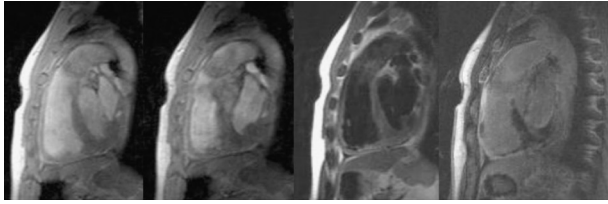


Figure 2.

examination. The electrocardiogram (EKG) showed epsilon wave in leads V1–V3.

Echocardiogram showed enlargement and severe dysfunction of the right ventricle and presence of micro aneurysms. He was undergone stress testing and developed an episode of non-sustained ventricular tachycardia (VT). Pt 2: Patient was hospitalized after an episode of syncope and it was detected sustained VT (LBB pattern), converted to sinus rhythm after electrical cardioversion. EKG showed a sinus rhythm, incomplete right bundle block and signs of electrical inactivity in inferior. Echocardiogram showed enlargement and severe dysfunction of RV and presence of hypokinesia in inferior wall. Patients performed signal-averaged EKG and in both it was found the presence of late potentials. CMR was performed at this time. In these two patients we detected the presence of myocardial fibrosis, with predominant involvement of RV (Figure 1), but concomitant presence of areas of delayed enhancement in septum, anterior wall and inferior wall (Figures 2 and 3).

The patients were referred to electrophysiological study. In pt 1, it was induced sustained VT with Left Bundle Block (LBB) pattern and it was not in case 2, who was in regular use of amiodarone. Patients were referred to a cardioverter-defibrillator implantable.

Conclusions: Gadolinium-enhanced CMR could detect the presence of a pattern of patch myocardial fibrosis with a major involvement of RV in 2 patients with clinical diagnosis of ARVD/C and malignant ventricular arrhythmias. These findings may have implications to improve early diagnosis and risk stratification of ARVD/C.

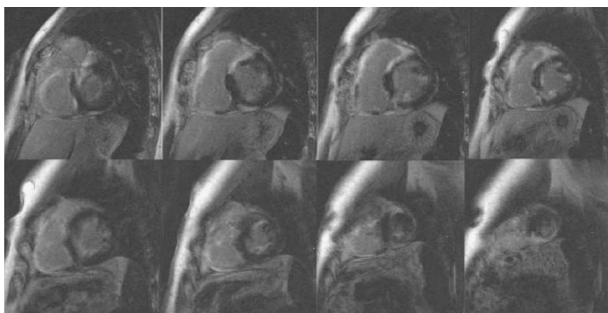


Figure 3.

340. Altered 3D LV Systolic Strain and Strain Rate by MR Tissue Tagging in Type 2 Diabetes Mellitus Patients with Diastolic Dysfunction and Normal Ejection Fraction

Carissa G. Fonseca,¹ Ajith M. Dissanayake,² Robert N. Doughty,¹ Gillian A. Whalley,¹ Greg D. Gamble,¹ Brett R. Cowan,¹ Christopher J. Occleshaw,³ Alistair A. Young.¹ ¹Faculty of Medical and Health Sciences, University of Auckland, Auckland, New Zealand, ²Middlemore Hospital, South Auckland Health, Auckland, New Zealand, ³Department of Cardiac Radiology, Green Lane Hospital, Auckland, New Zealand.

Introduction: Type 2 diabetes mellitus (DM) is associated with excess cardiovascular morbidity and mortality. Significant diastolic dysfunction is often found in DM patients in the absence of atherosclerotic coronary artery disease (CAD) and regional wall motion anomalies. However, there is little information regarding 3D systolic and diastolic strain in this patient group.

Purpose: To non-invasively assess both systolic and diastolic 3D myocardial strain in type 2 DM patients with normal ejection fraction and diastolic dysfunction.

Methods: 28 patients (age 33–70 years) with a history of type 2 DM and evidence of diastolic dysfunction with no regional wall motion anomalies on screening echocardiogram, together with 31 normal healthy volunteers (NV, age 19–74 years), with no evidence of cardiac disease, were examined with multislice cine anatomical and tagged MRI. Three-dimensional analysis of the images enabled comparison of mitral valve plane (MVP) motion, LV circumferential and longitudinal strain and torsion, and strain relaxation rates. Pulsed wave Doppler echocardiography of mitral inflow and tissue Doppler imaging of the mitral annulus identified diastolic dysfunction in all patients.

Results: LV ejection fraction was normal in both patients and volunteers. LV mass:EDV ratio was increased in the diabetics. Tagged MRI showed a reduction in the diabetics, compared with NV, in peak systolic MVP displacement (1.06 ± 0.24 patients vs. 1.21 ± 0.28 cm NV, $p=0.040$) and peak diastolic MVP velocity (4.66 ± 1.26 vs. 5.91 ± 1.12 cm/s, $p=0.008$). Peak circumferential strain (S_C) was also reduced (16.66 ± 1.99 vs. $19.46 \pm 2.44\%$, $p<0.001$), as was peak systolic S_C rate (88.16 ± 12.43 vs. $97.85 \pm 11.36\%/s$, $p=0.008$) and peak diastolic S_C relaxation rate (70.83 ± 19.84 vs. $108.26 \pm 40.88\%/s$, $p<0.001$). Peak longitudinal strain (S_L) was reduced (12.54 ± 2.19 vs. $16.15 \pm 2.11\%$, $p<0.001$) and decreases were also observed in peak systolic S_L rate (69.12 ± 14.36 vs. $80.74 \pm 10.64\%/s$, $p=0.003$) and peak diastolic S_L relaxation rate (62.51 ± 21.11 vs. $91.67 \pm 36.47\%/s$, $p=0.003$).



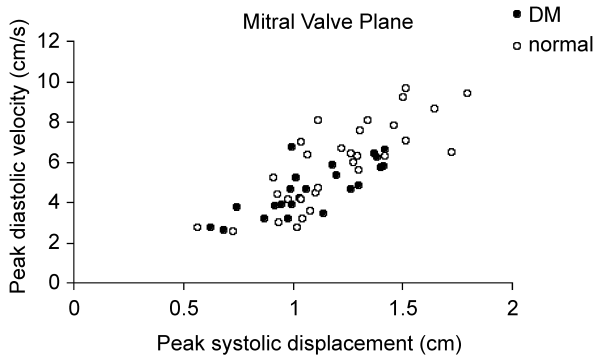


Figure 1. Relationship between peak systolic MVP displacement and peak diastolic MVP velocity.

$p < 0.001$). Peak systolic torsion was increased in the diabetics (6.80 ± 1.44 vs. 5.82 ± 1.26 degrees, $p = 0.025$) as was peak systolic rate of change of torsion (36.02 ± 7.47 vs. 29.87 ± 5.36 degrees/s, $p = 0.002$). However, there was no difference in peak diastolic relaxation of torsion (34.09 ± 10.597 vs. 34.17 ± 9.27 degrees/s, $p = \text{NS}$). In both patients and normal volunteers, significant correlations were observed between the peak rate of relaxation and the peak systolic value of each of the parameters examined (MVP motion; Figure 1, S_C , S_L and torsion: $r > 0.5$, $P < 0.01$ in both patients and NV).

Conclusions: Systolic as well as diastolic myocardial strain and strain-rate, as measured by 3D MR tissue tagging, is impaired in type 2 DM patients with normal ejection fraction and diastolic dysfunction. Our study highlights the need to take into account both tissue behaviour and LV hemodynamics when assessing LV function.

341. The Clinical Significance of a Common, Functional, X-Linked Angiotensin II Type 2-receptor Gene Polymorphism (–1332 G/A) in Patients with Hypertension

Khaled Alfakih,¹ Azhar Maqbool,² Gavin Bainbridge,¹ John Ridgway,¹ Anthony Balmforth,² Alistair Hall,³ Mohan Sivananthan.¹ ¹Cardiac MRI unit, Leeds General Infirmary, Leeds, United Kingdom, ²Institute of cardiovascular research, University of Leeds, Leeds, United Kingdom, ³Academic Unit of cardiovascular medicine, Leeds General Infirmary, Leeds, United Kingdom.

Purpose: We evaluated the common intronic polymorphism (–1332 G/A) of the AT_2 receptor gene (X-chromosome) for an association with left ventricular hypertrophy (LVH), as measured by cardiac MRI.

Methods: Sixty normal volunteers were studied to establish normal ranges for cardiac MRI as well as the frequency of the gene in the normal population. 205 patients with hypertension were also studied. MRI studies were performed on a 1.5-Tesla Philips system using a cardiac phased-array coil with breath holding. Multiple short axis slices, covering the entire heart were acquired using a TGE pulse sequence (TR=8.8 ms, TE=5.2 ms, flip angle=35°). Contour tracing of the LV at end diastole was performed off-line using MASS software. Following DNA extraction, a 310 bp fragment of DNA containing the AT_2 (–1332 G/A) polymorphic site was amplified by PCR. Restriction fragment length polymorphism analysis was performed to identify the G allele which digested into two bp fragments. Means and standard deviations were calculated for LV mass indexed to body surface area (BSA), for volunteers and patients.

Results: The mean LV mass indexed to BSA for the male volunteers was 77.8 ± 9.1 g/m² (n=30), female volunteers was 61.5 ± 7.5 g/m² (n=30), male patients was 94.3 ± 19.6 g/m² (n=125), female patients was 71.2 ± 12.0 g/m² (n=75). 73 (37.1%) of all patients had elevated LV mass index, defined as the mean LV mass index for normal volunteers plus two standard deviations. Chi-square comparison of normotensive volunteers without LVH (NT LVH-) and hypertensive patients with LVH (HT LVH+) recorded a difference in genotype frequency (A/AA vs. G/GG) that was significant ($p = 0.023$) (Fig. 1).

Conclusions: We observed an association between the AT_2 (–1332 G) allele and the presence of LVH in hypertensive subjects.

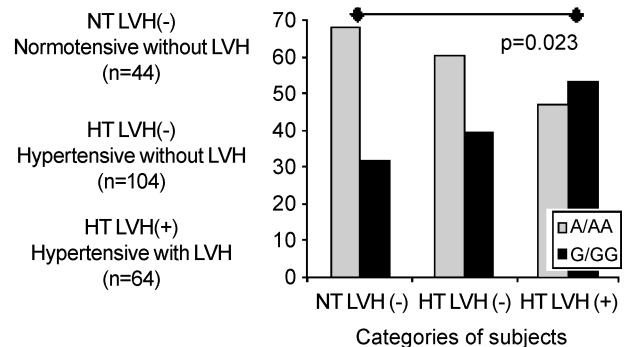


Figure 1.



342. Pulmonary MR Venography Facilitates Electrophysiologic Pulmonary Venous Ablation

Jeremy D. Collins, BS,¹ David Bello, MD,² Timothy Betts, MD,² Eugene Huo, BS,¹ Stephanie Shors, MD,¹ James Carr, MD,¹ F. Scott Pereles, MD.¹ ¹Radiology, Feinberg School of Medicine, Northwestern University, Chicago, IL, USA, ²Cardiology, Feinberg School of Medicine, Northwestern University, Chicago, IL, USA.

Introduction: Pulmonary Magnetic Resonance angiography (MRA) generates high-resolution images of the pulmonary veins (PV) and left atrium (LA), permitting characterization of complex PV anatomy. Indications for Pulmonary MRA include electrophysiologic PV ablation, a proven technique for the treatment of paroxysmal atrial fibrillation (PAF). Three-dimensional (3D) MRA datasets can be volume-rendered to provide high-resolution models of PV and LA anatomy. Knowledge of complex PV anatomy prior to PV ablation may facilitate ablation and decrease fluoroscopy time. Conventional pulmonary venography for characterization of PV anatomy is less desirable than MRA because it is invasive, requires nephrotoxic iodinated contrast, and yields 2D data with low contrast resolution.

Purpose: To determine if pre-ablative pulmonary MR venography with intra-ablative viewing facilitates PV ablation by reducing fluoroscopy time.

Methods: At 1.5T (Magnetom Sonata, Siemens Medical Solutions, Malvern, PA) we studied the morphology of the LA and PV with breath-held gadolinium-enhanced 3D MRA 13 patients (age 53±8 years) with PAF undergoing PV ablation. Contrast kinetics were determined with a time-resolved 3D FLASH MRA sequence with temporal resolution of 5 seconds. MRA sequence parameters were TR/TE 1.8/0.7, flip angle 13°, 87.5% rectangularized 380 cm FOV, and 30–40 partitions of 2.2–2.7 mm thickness with mean in-plane resolution of 1.8 mm×1.5 mm and mean voxel volume of 7 mm³. Fifteen ml of Gd-DTPA (Berlex Magnevist, Wayne, NJ) was administered at 3.0 ml/s followed by a 20 ml saline flush also at 3 ml/s. 3D data volumes were serially acquired out to 30 seconds, producing an initial mask acquisition and 5 contrast-enhanced time-resolved datasets. These lower spatial, but high temporal, resolution images were followed by a high spatial resolution pulmonary MRA of the following parameters: TR/TE 2.9/1.1, flip angle 13°, 87.5% rectangularized 380 cm FOV, and 60–72 partitions of 1.2–1.5 mm thickness with mean in-plane resolution of 1.8 mm×1.5 mm and voxel

volume of 3.5 mm³. 30 ml of Gd-DTPA was administered at 3.0 ml/s with a 20 ml saline flush also at 3 ml/s. Central lines of k-space were acquired upon contrast arrival in the PV. MRA data was volume rendered (VR) on a stereoscopic workstation (Virtuoso, Siemens Medical Systems, Iselin, NJ). PV ostial diameter and cross-sectional area measurements were obtained on multi-planar reformatted (MPR) images. VR MRA datasets were converted into digital movies and were viewed on a laptop computer in the electrophysiology lab adjacent to real-time fluoroscopic images. MPR MRA-determined ostial dimensions were available intra-operatively to facilitate fluoroscopic vein identification and contact mapping balloon sizing. Fluoroscopy times were compared for patients undergoing pre-ablative MRA mapping and a cohort of 22 consecutive patients (age 57±9 years) diagnosed with PAF who underwent catheter ablation without pre-ablative MRA planning.

Results: There was a significant difference in both ostial diameters and ostial cross-sectional area between each vein (ANOVA, p=0.003 and p<0.005 respectively). Mean EP PV ablation fluoroscopic time with MRA planning versus fluoroscopic imaging alone were 85±20 minutes and 114±20 minutes respectively. Pre-ablative MRA planning resulted in a significant mean fluoroscopy timesavings of 26% (p<0.05).

Conclusions: In patients with PAF undergoing PV ablation, analysis of MRA datasets depicting PV anatomy confirms that there is great variability in anatomy between veins. Pre-ablative 3D PV mapping by MRA facilitates fluoroscopic identification of individual veins and significantly reduces fluoroscopic radiation time.

343. Subclinical Pulmonary Vein Narrowing is Common Following Atrial Fibrillation Ablation

Thomas H. Hauser, MD,¹ Susan B. Yeon, MD, JD,¹ Seth McClennen, MD,¹ George Katsimaglis, MD,¹ Kraig V. Kissinger, RT, MS,¹ Mark E. Josephson, MD,¹ Neil M. Rofsky, MD,² Warren J. Manning, MD.¹ ¹Medicine, Cardiovascular Division, Beth Israel Deaconess Medical Center, Boston, MA, USA, ²Radiology, Beth Israel Deaconess Medical Center, Boston, MA, USA.

Introduction: Radiofrequency ablation (RFA) for the treatment of atrial fibrillation (AF) is increasingly per-

formed. While clinical pulmonary vein (PV) stenosis is a rare complication of these procedures, subclinical narrowing may be more common.

Purpose: We assessed potential changes in PV size following AF ablation using contrasted enhanced 3D magnetic resonance angiography (MRA).

Methods: Maximal PV diameter, circumference and cross-sectional area (CSA) were measured in a group of consecutive patients who underwent PV MRA before and 1.3 months after their first AF ablation. The number and duration of RFA during the index procedure were also recorded.

Results: There were a total of 86 PV in 23 patients (20 [87%] men, age 54 ± 11 years). There were significant decreases in maximal PV diameter (21 ± 6 to 19 ± 5 mm), circumference (57 ± 14 to 52 ± 13 mm) and CSA (236 ± 118 to 194 ± 92 mm²; $p < 0.001$ for all) from baseline to follow-up studies. No PV diameter reduction of $\geq 50\%$ was seen, although 7 (8%) PV had a diameter reduction of $\geq 25\%$ and $< 50\%$. In comparison, 9 (11%) PV had a $\geq 50\%$ CSA reduction and 16 (19%) PV had a 25% to 49% CSA reduction. The reduction in PV size was not related to either the number of RFA per PV (median=8) or the RFA duration (median=210 s, $p > 0.1$ for all measures of PV size).

Conclusions: Although clinical PV stenosis is rare, subclinical PV narrowing is common after RFA for the treatment of AF with the greatest reduction in CSA. The severity of PV narrowing appears unrelated to the intensity of RFA and may be related to absence of AF and/or hemodynamic changes such as decreased left atrial pressure.

344. Systolic Torsion Modification in Response to Aortic Valve Replacement in Advanced Aortic Stenosis Patients: An MRI Systolic and Diastolic Torsion Study Using HARP

Robert W. W. Biederman, MD,¹ June Yamrozik,¹ Ronald B. Williams,¹ Geetha Rayarao,¹ Maria Jaksec,¹ Diane A. Vido,¹ Sunil Mankad, MD,¹ James A. Magovern, MD,¹ Nathaniel Reichek, MD,² Nael Osman, PhD,³ Mark Doyle, PhD.¹ ¹Allegheny General Hospital, Pittsburgh, PA, USA, ²St. Francis Hospital, Roslyn, NY, USA, ³Johns Hopkins University, Baltimore, MD, USA.

Background: Compensatory left ventricular hypertrophy in Aortic Stenosis (AS) alters the manner in which circumferential and meridional myocardial fibers interact. Prior to end-stage AS, contractile performance and torsion become supranormal. However, at the level of the myocyte there is paradoxical contractile dysfunction. This disconnect is manifest due to the ability for hypertrophied sarcomers in parallel to minimally contract, yet due to their combined thickening, effect substantial endocardial excursion. Nonetheless, when evaluated in terms of an energy model, substantial Work is expended by the hypertrophied heart to eject blood and to produce abnormally high degrees of torsion.

Hypothesis: We hypothesized that following aortic valve replacement (AVR), the work (cardiac work index Cwi) expended by the LV to eject blood is preserved, while the energy component directed towards producing torsion (Torsion Energy Index, TEi) is beneficially reduced.

Methods: Seventeen (17) patients with late, but not decompensated, AS underwent MRI with tissue tagging (GE CV/i). Torsion analysis was performed using an automated software program, HARP (Diagnosoft). Work was calculated as was the TEi for each slice as the area under the rotation-time plots output from HARP. Data were compared pre to post AVR (6.1 ± 1.1 mo).

Results: Following AVR, LV mass (LVM) decreased, (187 ± 61 g vs. 160 ± 47 g, $p < 0.005$), as did LVM/vol (1.62 ± 0.64 vs. 1.28 ± 0.32 g/ml, $p < 0.05$). However, no change was noted in the CWi (12116 ± 4407 vs. 12605 ± 2833 ml-mmHg, $p = \text{ns}$) or EF (68 ± 17 vs. 67 ± 8 , $p = \text{ns}$). Both pre and post AVR, the maximum torsion attained increased linearly from base to apex ($p < 0.001$). At the apex, where maximal torsion was realized, the TEi decreased following AVR (5958 ± 1957 vs. 4290 ± 1725 , $p < 0.05$). However, the rate of torsion generation was maintained pre to post AVR (0.074 ± 0.031 deg/ms vs. 0.065 ± 0.031 deg/ms, $p = \text{ns}$).

Conclusion: In Aortic Stenosis, LV torsion is supranormal, being driven primarily by apical rotation. Following AVR, the rate of torsion production at the apex is maintained, while the torsional energy index (TEi) is reduced. As well, indices of ventricular function such as EF and CWi are maintained following AVR surgery. Thus, the benefit of AVR is manifested at the level of the myocardium, which experiences a reduced torsional work load.

In toto, LV myocardial mechanical efficiency is improved following AVR. When combined with the mass regression following AVR, further reductions in baseline energy requirements of the myocardium are evident.



**345. LV Diastolic Dysfunction:
A Cardiovascular MRI Quantitative
Comparison with Echocardiography**

Vikas K. Rathi, MD, Mark Doyle, PhD, June Yamrozik, Ronald B. Williams, Craig Truman, Maria Jaksec, Diane A. Vido, Robert W. W. Biederman, MD. Allegheny General Hospital, Pittsburgh, PA, USA.

Introduction: Cardiovascular MRI (CMR) image quality (spatial resolution, intrinsic 3D nature and reproducibility) has demonstrable superiority compared to echocardiography (TTE) for systolic function. However, to date no systematic assessment of diastolic function representing a wide range of lusitropic perturbations has been performed by CMR. Limitations in the current assessment of diastolic function by TTE exist, including user dependence, acoustic window, cosine errors and the inability to interrogate flow in X, Y, and Z coordinates and yet, TTE is regarded as the de facto “gold standard.”

Hypothesis: We hypothesize that CMR diastolic flow data is comparable to TTE but without its acquisition limitations.

Methods: In 21 subjects (male:15, age:26–76 and female:6, age:46–76) including 7 controls underwent optimized CMR phase velocity mapping using CV/i 1.5 GE CVMRI scanner (Milwaukee, WI). The 14 patients had diverse diastolic pathology including 6 with impaired relaxation, 2 with restrictive, 2 pseudo-normalization and 3 with EA fusion and the re-

maining was normal. To include complete diastole, 60 phases/cycle providing a mean temporal resolution of 19 ± 3 ms was used to sample 1) entire mitral valve plane in 3D 2) cross-section through right upper pulmonary vein (most often visualized by TTE). By design, within 2 hr post CMR, a blinded TTE of MV and PV by pulsed wave Doppler on Phillips Sonos 5500 (Andover, MA) using ASE guidelines was obtained. CMR calculated peak mitral early ‘E’ and late atrial systolic ‘A’ velocities, pulmonary vein velocities, E/A ratios, E gradients and deceleration time (DT) were compared with the means of 4 TTE images (see Table 1).

Results: All of the mitral and pulmonary vein inflow patterns were imaged by CMR while only 17 out of 21 pulmonary veins were imaged by TTE and, thus the latter were not further analyzed. There was no significant difference in the total acquisition plus offline processing time by either technique. Morphologically, CMR correctly identified the mitral inflow abnormality with 100% correlation between CMR and TTE. Quantifying the absolute inflow velocities demonstrated that the E velocities, E gradients and DT by CMR and TTE were not statistically different. The lower amplitude mitral valve A velocities by CMR, however, were less than the TTE quantitated velocities. Consequently the absolute E/A ratios did not correlate. However, the morphologic representation of the E and A velocities were identical (Figure 1).

Conclusions: CMR phase velocity mapping has ability to derive diastolic function indices. Morphologically,

Table 1. Comparative mean data from CMR and TTE.

TTE	CMR	TTE	CMR	TTE	CMR	TTE	CMR	TTE	CMR
E _{Vel} Cm/Sec		A _{Vel} Cm/Sec		E/A		E _{Grad} mmHg		Dec _T msec	
77.45	71.14	55.52	40.83	1.6	2.0	2.63	2.13	157	154
(SD±24)	(SD±20)	(SD±16.4)	(SD±16.6)	(SD±0.76)	(SD±0.97)	(SD±1.6)	(SD±1.3)	(SD±43.6)	(SD±47.1)
p=0.07		p=<0.05		p=<0.05		p=0.06		p=0.8	

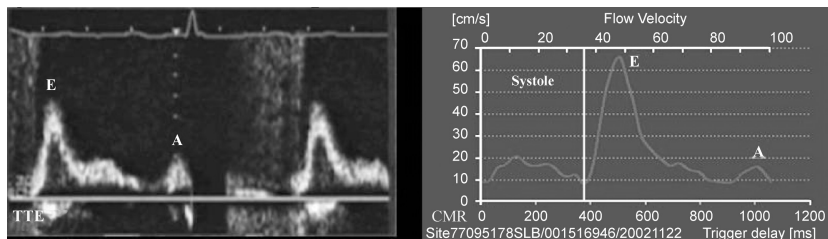


Figure 1. Restrictive flow pattern with short DT and high E/A ratio. (View this art in color at www.dekker.com.)

there is homology between the CMR and TTE derived diastolic flow representations despite heterogeneous pathology, with near exact inflow E velocity quantification. Given the advantages CMR provides for systolic determinations without the TTE limitations, diastolic applications appear equally possible.

346. Preclinical Dystrophin Deficient Cardiomyopathies Manifest Abnormal Segmental Myocardial Torsion

Marvin W. Ashford, Jr., MD,¹ Xin Yu, ScD,¹ Wei Liu, MS,² Katherine A. Lehr, RN,¹ Mary P. Watkins, RT,¹ Todd A. Williams, RT,¹ Paul Abraszewski, MD,¹ Shioh J. Lin, MS,¹ Anne Connolly, MD,³ Samuel A. Wickline, MD.¹ ¹Cardiovascular Medicine, Washington University, St. Louis, MO, USA, ²Biomedical Engineering, Washington University, St. Louis, MO, USA, ³Pediatrics, Washington University, St. Louis, MO, USA.

Introduction: Duchenne muscular dystrophy (DMD) is an X-linked disorder characterized by early onset of skeletal muscle degeneration and progressive weakness. Although cardiomyopathy may occur in adolescence, it is often undetected due to physical inactivity and debility. We hypothesize that subtle defects in regional contractile function may be detected more sensitively at rest with cardiac magnetic resonance (CMR) by measuring segmental myocardial torsion.

Purpose: The purpose of this investigation was to apply the method of CMR tagging to uncover evidence of early cardiac dysfunction in young subjects with DMD.

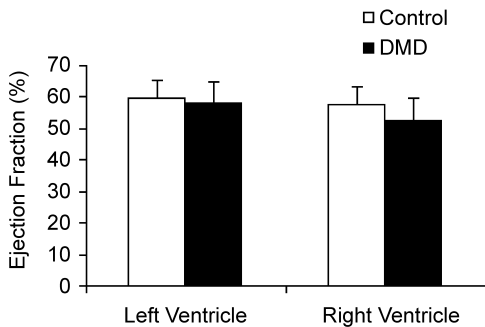


Figure 1. Left and right ventricular ejection fractions.

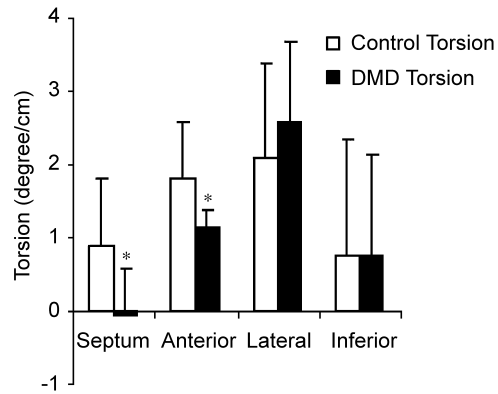


Figure 2. Segmental torsion.

Methods: Seven DMD patients without known heart disease and eight age-matched healthy males were recruited from a pediatric clinic at Washington University Medical Center. All subjects were evaluated using a 1.5 tesla scanner. Cine images of contiguous short-axis planes from the mitral valve plane to the apex were obtained using an ECG-triggered gradient-echo sequence: repetition time (TR), 3.3 msec; echo time (TE), 1.65 msec; flip angle (FA), 50 degrees; field of view (FOV), 400 mm; acquisition matrix 224X256; and slice thickness (t), 10 mm. Apical, mid-ventricular, and base short-axis slices were tagged by applying two orthogonal spatial modulations of magnetization pulses at end-diastole. The tagging gradient was 10 Gauss/cm with a pulse delay of 0.2 msec, which yielded a tag grid spacing of 0.6 mm. Tag displacement was tracked throughout the cardiac cycle by acquiring gradient echo cine images: TR, 25 msec; TE, 4.9 msec; FA, 13 degrees; FOV, 330 mm; acquisition matrix, 176X256; and t, 8 mm. Regional myofiber twist was measured in four walls (anterior, septum, inferior, and lateral) using a MATLAB-based computer program developed in our laboratory. Ventricular torsion was computed by normalizing the global twist by the distance from apex to mitral valve plane. Student's t-test was used to test for differences between the control and DMD groups.

Results: No significant differences were observed between control and DMD groups with respect to age (11.8 years versus 11.4 years), left ventricular ejection fraction (58.4% versus 59.5%), right ventricular ejection fraction (52.6% versus 57.4%), left ventricular mass (101.2 grams versus 94.4 grams), and right ventricular mass (60.6 grams versus 59.7 grams), respectively (see Figure 1). Figure 2 indicates that

the septal and anterior walls exhibit reduced torsion in the DMD group ($p < 0.05$). Torsion in the lateral and inferior walls is equal. A trend toward decreased global torsion was observed in DMD patients ($p = 0.14$).

Conclusion: In patients predisposed to genetic cardiomyopathies due to mutations of structural genes, occult cardiac dysfunction can be measured regionally with CMR tagging. We suggest that the assessment of torsion may provide a tool to quantify disease progression and to evaluate over time therapies designed to treat incipient heart failure.

347. The Benefit of Aortic Valve Replacement for Aortic Stenosis on LV Mechanics is Reduced by CAD

Robert W. W. Biederman, MD,¹ Mark Doyle, PhD,¹ June Yamrozik,¹ Ronald B. Williams,¹ Diane A. Vido,¹ Maria Jaksec,¹ Sunil Mankad, MD,¹ James A. Magovern, MD,¹ Nathaniel Reichek, MD.² ¹Allegheny General Hospital, Pittsburgh, PA, USA, ²St. Francis Hospital, Roslyn, NY, USA.

Background: In patients with severe aortic stenosis (AS), considerable effort has been expended to understand the mechanism of improvement following aortic valve replacement (AVR). While results following AVR have been very encouraging, the actual effects regarding the presence or absence of CAD (CAD+, CAD-) are not well understood. Yet, they are important as the population eligible for benefit increases as surgical and medical understanding develops.

Hypothesis: We hypothesized that the presence of CAD blunts the beneficial effects of reverse remodeling following AVR for AS.

Methods: Twenty patients (61–90 years, 10 female) with severe AS underwent MRI pre AVR and 6.1±1.2 months post AVR. LV mass Index (LVMI), mass/volume (LVMI/vol) and EF were measured, along with 1D transmural circumferential intramyocardial strain (%S). Complete pre and post data was available in 16 pts.

Results: EF was normal and similar in the two groups at baseline and remained unchanged pre to post AVR (69±17 vs. 67±8%, $p = \text{NS}$). However, LVMI and LVMI/vol were decreased after AVR, indicating that reverse remodeling occurred (101±29 vs. 83±23 g/m², $p < 0.001$; 1.6±0.6 vs. 1.3±0.3, $p < 0.005$). On sub-set analysis, the reduction in LVMI and LVMI/vol

was confined *only* to CAD-patients ($p < 0.05$). Pre AVR, %S was similar in the CAD- and CAD+ subgroups (21±5 vs. 21±9) and mean %S trended higher for the entire group after AVR (21±4 to 23±5%, $p = \text{NS}$). However, while improvement was noted in the CAD- subgroup (21±5 to 25±5%, $p < 0.05$), none was observed in the CAD+ subgroup (21±9 to 19±4, $p = 0.19$).

Conclusion: Following AVR for AS, LV mass regression is observed, while EF, which was in the normal range pre AVR, remains unchanged. We note that the majority of benefit is experienced by patients without CAD, with regard to LV mass regression and %S improvement. Interestingly, pre AVR %S was similar in patients with and without CAD. Following AVR, patients with CAD trended towards decreased intramyocardial function. The relationship to long-term outcome of short-term reverse remodeling and improved intramyocardial function remains to be determined.

348. Normal Human Left Ventricular Dimensions Using Steady State Free Precession MRI in the Radial Long-Axis Orientation

Sarah R. Clay, BSc, Khaled Alfakih, MBBS, Alexandra Radjenovic, MSc, Timothy Jones, MSc, John P. Ridgway, PhD, Mohan U. Sivanathan, PhD. *BHF Cardiac MRI Unit, Leeds General Infirmary, Leeds, United Kingdom.*

Introduction: The radial long-axis orientation has been shown to have intrinsic advantages over the short-axis orientation due to improved contrast, and the avoidance of errors related to basal slice determination, both of which aid image analysis (Bloomer et al., 2001). Previous work has highlighted the need for technique specific normal ranges (Table 1, Figure 1).

Purpose: The purpose of this study was to establish normal ranges of left ventricular (LV) dimensions for the radial long-axis orientation.

Methods: Forty normal subjects (20 male, average age 32.3, age range 19 to 58; 20 female, average age 37.4, age range 21 to 54) were examined and a steady state free precession (SSFP) pulse sequence, the technique of choice in this orientation, was used to obtain 8 radial slices. Two observers using MASS software traced endocardial and epicardial contours independently and volumetric analysis was carried out

Table 1. The mean values ± one standard deviation and the normal range for LV parameters.

	Male		Female	
	Mean ± SD	Normal range	Mean ± SD	Normal range
EDV (ml)	181.1 ± 30.3	121–242	144.9 ± 21.1	103–187
EDV/BSA (ml/m ²)	90.9 ± 14.3	62–120	80.7 ± 11.2	58–103
ESV (ml)	70.7 ± 18.0	35–107	52.5 ± 12.4	28–77
Mass (g)	136.2 ± 20.5	95–177	96.2 ± 15.5	65–127
Mass/BSA (g/m ²)	68.0 ± 8.8	50–86	53.7 ± 8.9	36–72
EF (%)	61.1 ± 6.0	49–73	63.6 ± 4.8	54–73

Key: SD=standard deviation; EDV=end diastolic volume; BSA=body surface area; ESV=end systolic volume; EF=ejection fraction.

using a validated program developed in the department specifically for the radial long-axis orientation. A similar program has recently been implemented and validated in the research version of the MASS software and this feature is to be added to the commercially available version in the near future.

Results: The observer variability for LV mass and LV EDV were expressed as the standard deviation of the difference between two values (SDD). The inter-observer variability for LV mass and LV EDV was 6.8 and 7.0 respectively and the intraobserver variability was 5.7 and 4.5 respectively. These values were lower than data recently published for a normal range in the short-axis orientation using SSFP (Alfakih et al., 2003).

Conclusions: A gender specific normal range in the radial long-axis orientation was established. These results have provided further evidence that measurements using radial images are more reproducible than in the short axis orientation.



Figure 1. A radial long-axis image taken at end-diastole. (View this art in color at www.dekker.com.)

REFERENCES

Alfakih, K., Plein, S., Thiele, H., Jones, T., Ridgway, J., Sivanathan, M. U. (2003). Normal human left and right ventricular dimensions for MRI as assessed by turbo gradient echo and steady-state free precession imaging sequences. *J. Magn. Reson.* 17:323–329.

Bloomer, T., Plein, S., Radjenovic, A., Higgins, D. M., Jones, T. R., Ridgway, J. P., et al. (2001). Cine MRI using steady state free precession in the radial long axis orientation is a fast accurate method for obtaining volumetric data of the left ventricle. *J. Magn. Reson.* 4:685–692.

349. Clinical Value of CMR for the Detection of Pericardial Fat in Patients with a False Diagnosis of Effusion by Echocardiography

Ana G. Almeida, MD, PhD, Miguel Pacheco, MD, Eduardo I. Oliveira, MD, Pedro N. Marques, MD, Claudio David, MD, Arminda Veiga, MD, Sandra Rodrigues, M-Celeste Vagueiro, MD, PhD. *Cardiology, University Hospital Santa Maria, Lisbon, Portugal.*

Introduction: Pericardial effusion is a frequently detected condition by echocardiography and, very often, represents a diagnostic challenge. Echocardiography, however, isn't often able to distinguish between pericardial fluid and fat and, so potentially, misdiagnose an effusion.

Purpose: The aim of this study was to assess the clinical role of CMR in the detection of pericardial fat in patients with the echocardiographic diagnosis of pericardial effusion.

Methods: We evaluated, retrospectively, 100 CMR consecutive studies of our case-load, with miscellaneous conditions (valvular and ischemic heart disease, cardiomyopathy, pericardial effusion, aortic diseases, cardiac masses) and the diagnosis of pericardial effusion, as assessed by previous echocardiography. The following variables were analysed: presence of pericardial effusion vs. fat; size of fluid or fat at the level of each cardiac wall in comparison with echocardiographic findings, considering three degrees of severity (mild, moderate, severe); size (mm) of the pericardial abnormality at the level of free right ventricle wall and the posterior left ventricle wall. CMR diagnosis of pericardial fluid was based on the presence or absence of signal in the pericardial space on SE T1 images and bright signal on cine-MR, while fat was diagnosed by the occurrence of bright signal on T1 images, reduction of intensity by fat-suppression sequence and low signal around the heart by cine-MR. Axial and short-axis planes were always obtained. A 1.5 Tesla machine was used (GE, Signa).

Results: 7 over 100 (7%) patients with the echocardiographic diagnosis of moderate pericardial effusion showed, by CMR study, absence of fluid and occurrence of a thick layer of pericardial fat, which was also associated to increased epicardial fat. In these patients, fat was present all around the heart, with a maximum thickness of 30 mm and a minimum of 22 mm. There was a 100% concordance between the two methods, concerning the distribution of the pericardial abnormality. There was no significant difference between the dimension of the pericardial abnormality (fluid/fat) over the right and posterior wall of left ventricle, obtained by CMR and echocardiography.

Conclusions: Although there is agreement between echocardiography and CMR, concerning dimensions and distribution of pericardial effusion/fat, CMR identified the presence of pericardial fat in an important number of patients with an echocardiographic false diagnosis of effusion. The clinical use of CMR in this condition is advantageous, since unnecessary further evaluation will be prevented.

350. Conventional Spin Echo Magnetic Resonance Imaging is Superior to Fast Spin Echo in Detection of Intramyocardial Fatty Infiltration

Suhny Abbara, MD, Raymond Q. Migrino, MD, David Sosnovik, Ricardo Cury, MD, Thomas J. Bra-

dy, Godtfred Holmvang. *Radiology, MGH, Boston, MA, USA.*

Background: Intramyocardial fatty infiltration (IMF) is a major criterion for arrhythmogenic right ventricular dysplasia (ARVD) and is associated with malignant arrhythmias. Because of lengthy duration of acquisition, free-breathing conventional spin echo (CSE) imaging of IMF has largely been supplanted by blood-suppressed breath-hold fast spin echo (FSE) techniques. However, the use of FSE, while advantageous because of shorter acquisition time, limits imaging of the RV to diastole. The aim of this study is to compare detectability of RV IMF using axial and sagittal CSE and sagittal FSE.

Methods: Thirty-two patients being evaluated for ARVD underwent cardiac gated MRI to evaluate for IMF. The patients were imaged in the prone position using a 30 cm phased array spine coil, and underwent axial and sagittal high resolution CSE and sagittal FSE imaging, with the following parameters: CSE: FOV 12–16 cm, slice thickness 5–7 mm, slice gap 1–1.5 mm, 256/160–224 frequency/phase encoding steps, 4 excitations, minimum echo time, repetition time equal to cardiac cycle length, spatial saturation pulses superior, inferior, posterior and over the atria; FSE: same FOV, trigger delay time of 400–600 ms, echo train length of 16–24, 256/192–224 frequency/phase encoding steps, 1 excitation). If an area of high intramyocardial signal intensity was detected, the sequence was repeated with fat suppression. Intramyocardial areas with high signal intensity that became hypointense following fat suppression were considered to be IMF. The 3 techniques were compared using McNemar’s chi square test.

Results: Axial CSE demonstrated fatty infiltration in 17 out of the 32 patients. Sagittal CSE only detected fat in 9 cases and sagittal FSE detected fat in only 3 cases (see Table 1, Fig. 1).

Conclusions: CSE is superior to FSE for detection of IMF, and axial CSE is superior to sagittal

Table 1. Detection of intramyocardial fatty infiltration.

	Fat present	Fat absent
I Axial CSE	17	15
II Sagittal CSE*	9	22
III Sagittal FSE ⁺	3	25

I vs. II: $p=0.02$ I vs. III: $P<0.001$ II vs. III: $P=0.03$.

*One patient without sagittal CSE.

⁺Four patients without FSE.

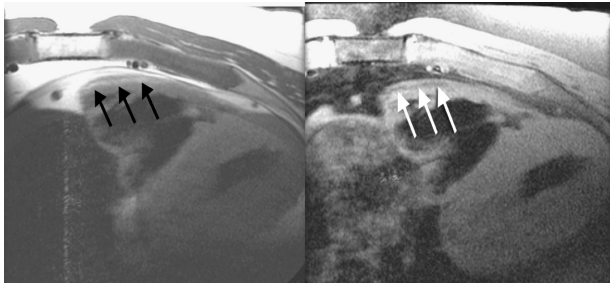


Figure 1.

CSE. The use of FSE results in underdetection of IMF and therefore may result in underdiagnosis of ARVD.

351. Validation of Improved Electrocardiographic Identification of Left Ventricular Hypertrophy in Women Using Cardiovascular Magnetic Resonance

Michael L. Chuang, MD, ScM,¹ Yoram Ariel, PhD,² Carol J. Salton, BA,¹ Kraig V. Kissinger, BS, RT (R) (MR),¹ Patricia A. Arand, PhD,³ Lois A. Goepfert, RN, MS,¹ Robert A. Warner, MD,³ Warren J. Manning, MD.¹ ¹Cardiovascular Division, Beth Israel Deaconess Medical Center, Boston, MA, USA, ²Inovise Medical, Inc, Boston, MA, USA, ³Inovise Medical, Inc, Newberg, OR, USA.

Introduction: The electrocardiogram (ECG) is commonly used to identify left ventricular hypertrophy (LVH). To date, electrocardiographic detection of LVH has been compared to M-mode or 2D echocardiography, the accuracies of which are decreased with anatomic factors such as poor echo windows or distorted ventricular shape in disease. The performance of the ECG for detection of LVH in a general population has not been compared with left ventricular mass measured using modern volumetric imaging

techniques. Additionally, the sensitivity of the ECG for LVH is lower in women than men.

Purpose: To assess the sensitivity, specificity and positive and negative predictive values of commonly used ECG algorithms for detection of LVH against mass determined using volumetric cardiovascular magnetic resonance (CMR) and to determine whether use of multiple gender-specific ECG criteria improves LVH detection in women.

Methods: 192 consecutive patients referred for evaluation of LV function, comprising 70 women and 122 men with a mean (SD) age of 50 (15) years, underwent CMR using a contiguous multislice SSFP breathhold cine technique (1.5-T Philips Gyroscan ACS/NT). Imaging parameters included TR=3.2 ms, TE=1.6 ms, FA=60 deg with 10-mm slice thickness and 1.92-mm² in-plane spatial resolution. Patients were classified as LVH+ or LVH- based on published CMR criteria (LV mass index; ≥ 74.7 g/m², women; ≥ 95.0 g/m², men). Immediately after CMR scanning, a 12-lead ECG was acquired from each patient using a standard clinical instrument (Mac Vu, Marquette Medical Systems). Multiple ECG criteria for LVH were compared to the CMR reference standard, including: Sokolow-Lyon (SL); gender-specific Cornell voltage (CV) and Cornell product (CP); 3 commercial algorithms (C1, C2, C3); and a novel ‘‘Audicor’’ algorithm that uses multiple gender specific criteria for LVH.

Results: Prevalence of CMR LVH was 13% in women and 23% in men (p=NS, chi-square test with Yates correction). Sensitivity (Sens,%) and specificity (Spec, %) for detecting LVH by gender for the various ECG criteria are shown in the Table 1, as are positive (PPV, %) and negative (NPV,%) predictive values. For ECG detection of LVH, the Audicor algorithm had the highest Sens and NPV in women, with preserved high specificity. For men all the ECG techniques were similar.

Conclusions: Commonly used ECG algorithms have high specificity regardless of gender but modest sensitivity for LVH in men and poor sensitivity in women. Use of multiple gender-specific ECG criteria for LVH improves sensitivity in women to a level comparable to that for men while maintaining high

Table 1. Performance of ECG algorithms vs. CMR for LVH.

	SL	CV	CP	C1	C2	C3	Audicor
Women: Sens/Spec	11/95	11/90	11/100	11/95	0/95	22/92	44/92
Men: Sens/Spec	50/85	33/99	61/90	46/82	46/81	68/82	54/90
Women: PPV/NPV	25/88	14/87	100/88	25/88	0/87	29/89	44/92
Men: PPV/NPV	50/85	91/84	65/89	43/84	42/84	53/90	63/87

specificity. Current ECG algorithms have been developed using M-mode echocardiography as the reference standard, although the cubed-power M-mode mass algorithms have been shown to overestimate LV mass relative both to volumetrically-determined mass and to necropsy results. In future it may be desirable to develop ECG algorithms for detection of LVH based on mass determined by CMR.

352. Rapid Phase Velocity Mapping of the Aortic Flow with and without SENSE-Volume and Velocity Measurements Compared to Standard Techniques

Srirama V. Swaminathan,¹ David L. Owen, RT,² Ian Paterson, MD,² Anthon R. Fuisz, MD.² ¹*Clinical Science, Philips Medical Systems, N.A., Cleveland, OH, USA,* ²*Cardiology, Washington Hospital Center, Washington, DC, USA.*

Introduction: Phase velocity mapping (pvm) sequences based on routine gradient echo technique (FFE) can be used to accurately measure blood flow in the aorta but are relatively time consuming. In the recent past faster techniques (Pruessmann et al., 1999) such as segmented k-space gradient echo technique (TFE) has been proposed. In this work we compared TFE based pvm sequences with and without SENSitivity Encoding (SENSE) (Chatzimavroudis et al., 2003) against the FFE technique. With the TFE technique there is a considerable reduction in acquisition time. The reduction in time is much more with SENSE combination.

Purpose: We hypothesized that TFE pvm could cut acquisition time without any loss in accuracy of volume measurements or velocity measurements.

Methods: 10 subjects, 7 of who are patients undergoing pvm for clinical purposes and 3 volunteers were studied. All the measurements were performed on Philips Intera CV (Philips Medical Systems, The Netherlands) system equipped with a 30 mT (150 T/m/s) Master gradient system. A five element SENSE Cardiac coil was used. TFE pvm sequences without and with SENSE (sTFE) were performed directly after standard pvm sequence. To establish the reproducibility the standard FFE pvm sequence, it was repeated before the TFE sequence. The regular FFE sequence used is a 2D Fast Field Echo (2D-FFE) with a TR/TE of 7.6/4.6 ms. A PC velocity of 250 cm/s was used and 2 signal averaging was done. A slice of 10 mm thick was planned axially. The average time of acquisition was

Table 1. FFE vs. TFE, sTFE and TFE vs. sTFE measurements.

	Flow volume (mL)	Peak velocity (cm/s)
FFE: Mean(SD)	68.53 (±22.42)	53.74 (±18.27)
TFE: Mean(SD)	72.15 (±35.25)	55.16 (±21.1)
STFE: Mean(SD)	71.06 (±25.54)	52.94 (±19.6)
FFE vs. TFE		
Difference: Mean(SD)	-3.63 (+30.43)	-1.42 (±5.97)
% Difference of mean	5.23%	2.64%
P value	0.36	0.24
FFE vs. sTFE		
Difference: Mean(SD)	-2.54 (±21.08)	0.8 (±8.06)
% Difference of mean	3.51%	1.45%
P value	0.36	0.38
TFE vs. sTFE		
Difference: Mean(SD)	1.09 (±25.97)	2.22 (±7.83)
% Difference of mean	1.53%	4.19%
P value	0.45	0.2

187 seconds for about 63 phases. The TFE sequence was then planned with the same parameter as FFE with TR/TE of 3.9/2.1 ms. 7 lines of k-space were acquired per TFE shot. For the SENSE acquisition a factor of 2 was used, with the same number of phases as the FFE sequence. Images were processed and volumes and velocities were calculated using Philips' Q-flow/S-track processing tool.

Results: Statistical analyses of the data from the two methods were performed. The results are summarized in Table 1. Paired T-test analysis was done and P<0.05 is considered significant. The range of mean difference in flow volume between three different techniques was -3.625 ml and 1.09 ml and peak velocities were -1.42 ml and 2.22 ml. Bland Altman analysis of the techniques was also performed. Figure 1 is a representative plot of the analysis between FFE and TFE. The percentage mean of difference of flow volume between TFE without and with SENSE and FFE are 5% and 3% respectively and is 1% between TFE with and without SENSE.

Conclusions: Statistical analysis of the flow volume and peak velocities from three different methods compares well. TFE technique cuts the acquisition time by about 80% as compared FFE and with SENSE it is reduced further by an additional 10%. This opens up the possibility of doing the acquisition under breathhold to minimize the respiratory artifacts. If one chooses, with SENSE one can acquire more

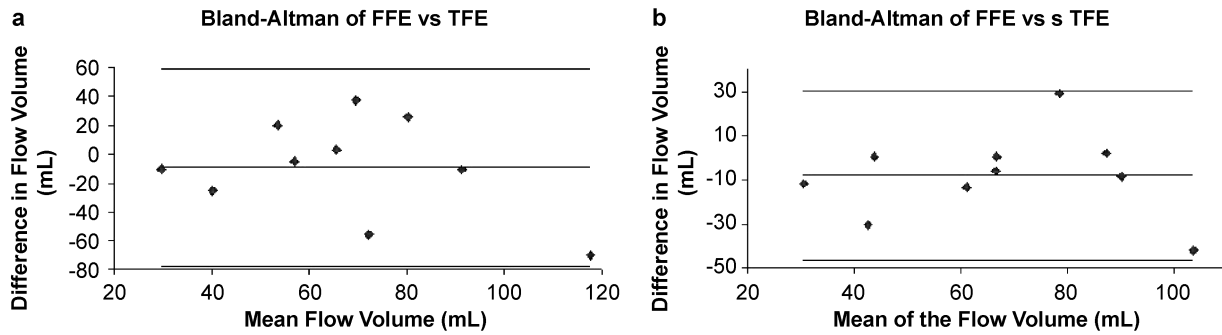


Figure 1. (View this art in color at www.dekker.com.)

phases. Hence an increased temporal resolution without any penalty in acquisition time. Shortening the acquisition time without negatively impacting accuracy allows the measurement of these important parameters to be more easily incorporated into clinical scans.

REFERENCES

Chatzimavroudis, G. P., Zhang, H., Halliburton, S. S., Moore, J. R., Simonetti, O. P., Schwartzman, P. R., Stillman, A. E., White, R. D. (2003). *J. Magn. Reson. Imaging* 17:65.
 Pruessmann, K. P., Weiger, W., Scheidegger, M. B., Boesiger, P. (1999). *Magn. Reson. Med.* 42:952.

353. Cardiovascular Magnetic Resonance in the Assessment of Aortic Regurgitation

Begoña Igual, MD,¹ Alicia M. Maceira, MD,¹ Vicente Miró, MD,² A Osa, MD,² Pilar López-Lereu, MD,¹ Joaquín Martín,¹ Jordi Estornell,¹ Miguel Palencia, MD.² ¹Eresa, Hospital La Fe, Valencia, Spain, ²Department of Cardiology, Hospital La Fe, Valencia, Spain.

Introduction: Phase contrast cardiovascular magnetic resonance sequences allow for the accurate assessment of aortic regurgitation (AR) but currently its clinical use is limited. In patients in whom other imaging techniques, as Doppler-echocardiography, are not feasible, CMR should be carried out if available.

Purpose: Our aim was to analyse the results of this technique in the assessment of AR severity compared to those derived from echocardiography, and also to evaluate the utility of aortic planimetry in the study of AR.

Methods: 30 consecutive patients with aortic valve disease referred for a cardiac MRI to assess ascending aorta diameters between January and April 2003 were included. The studies were performed with a General Electric® CVI (1.5 T) scanner. The study protocol included: 1) multislice dark blood (SSFSE) sequence in transverse orientation of the thorax to provide an overview of the cardiovascular anatomy, 2) FIESTA cine VLA, four -chamber and short-axis images to measure left ventricular mass and ejection fraction and 3) vascular phase-contrast sequences in three transverse planes across the aortic valve from which regurgitant orifice (RO, mm²) and regurgitant fraction (RF, %) were obtained. CMR criteria of AR severity: AR was classified as mild if regurgitant fraction (RF)<20%, moderate if RF=21–40% and severe if RF>40%. All patients also underwent Doppler-echocardiography within 2 weeks.

Results: Mean age was 65±11 yrs. Only 9 patients were females. In 11 cases (37%) the aortic valve was bileaflet. Pure aortic stenosis was found in 6 patients (20%), pure AR in 11 subjects (37%) and both aortic stenosis and regurgitation in another 13 (43%). CMR and Doppler-echocardiography showed good concordance in detection of significant AR (Kappa=0.67, P<0.01). CMR allowed for planimetry of the regurgitant orifice (see Table 1). There was a good correlation between RF and RO (r=0.84, P<0.01).

Conclusions: 1) Vascular phase contrast CMR sequence is a good method for evaluation of AR severity, with good concordance with doppler-echocardiography. 2) CMR planimetry of the regurgitant orifice

Table 1. RO according to AR severity.

	Mild AR	Moderate AR	Severe AR	P (ANOVA)
RF (%)	<20	21–40	>40	
RO (mm ²)	15±8	31±10	83±50	<0.001



is easy and simple, it provides useful information and should be done routinely in the CMR assessment of aortic regurgitation.

354. Efficacy of MR Indicators for Cardiac Resynchronization Therapy (CRT)

Benjamin England, MD, Cathleen Enriquez, Andrew Lee, Alexander P. Lin, Patrick Colletti, MD, Fernando Roth, MD, Mayer Rashtian, Mark Myers, MD, Brian D. Ross, MD, PhD. *Huntington Medical Research Institutes, Pasadena, CA, USA.*

Introduction: Cardiac resynchronization therapy (CRT) for treatment of resistant dilated cardiomyopathy (DCM) with disconjugate cardiac contractility (DCC) defined indirectly by ECG (qrs<130 ms), is beneficial in 68% but ineffective in 32% of patients (Abraham et al., 2002). Directly demonstrating DCC before treatment might improve outcome (Bax et al., 2002). MR is superior to echo in observing DCC and offers several means for its accurate quantitation (Enriquez et al., 2003).

Purpose: We evaluated three quantitative MR measures of DCC, asymmetry (I_s), asynchrony (I_a), and circumferential strain (ECC), with the principal aim of generating a robust numerical DCC index for use in future trials of CRT.

Methods and Patients: Standard cardiac MRI acquired on a 1.5T (GE LX 9.0) clinical MR scanner were analyzed by MASS (Medis Inc) and HARP (Diagnosoft Inc.). Figure 1 illustrates the principal indices of wall thickness (mm), mean maximum and minimum thickening (Δ) and asymmetry (ΔΔ), DCC indices I_a%=(ΔΔ/Δ)x100; I_a=%ΔΔ/Δ_{min} and asynchro-

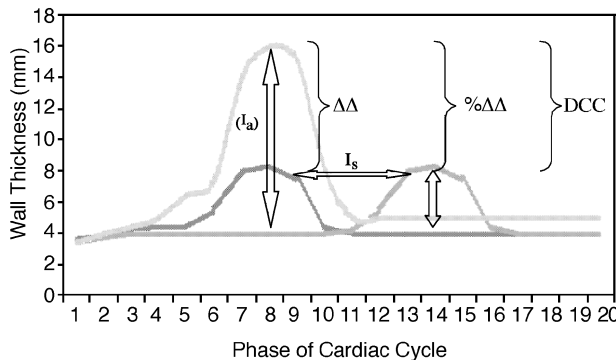


Figure 1. Measures of asymmetry (I_a) and asynchrony (I_s). (View this art in color at www.dekker.com.)

Table 1. Summary of LV function and wall motion analysis.

	Normal (11)	DCM (10)	CRT (4/10)
ΔΔ (mm)	4.44±1.8	3.26±2.5	2.60±1.6
% ΔΔ	36.9±14.9	107.2±60.6*	313.7±423.8
Asymmetry I _a	10.9±14.9	388.2±453.5*	275.0±259.8
Asynchrony Value	2.3±0.8	9.9±4.5*	9.0±2.9*
ECC (strain)	-14.6±3.3	-6.0±5.3**	1.8±2.6**

*p<0.05.
**p<0.005.

ny (A_s=peak Δ 1–2 ms). I_s was determined from the spread of phases over which individual segments of the left ventricle achieved their maxima, averaged over two short axis slices (Table 1).

DCC in tagged data was determined as circumferential strain, ECC, using HARP. The methods were evaluated in 10 DCM (EF<35%), 10 CRT candidates (EF<35%, QRS<120 ms, and 11 age-matched normal subjects, using t-test and standardized differences (SD=sd/diff; Power (N)=number of patients to reach P<0.05) to determine efficacy.

Results: Illustrative examples of normal, asymmetric and asynchronous wall motion are shown (Figure 2).

Measurements of asymmetry, asynchrony, and circumferential strain in left ventricular heart contraction distinguished control subjects from DCM patients in

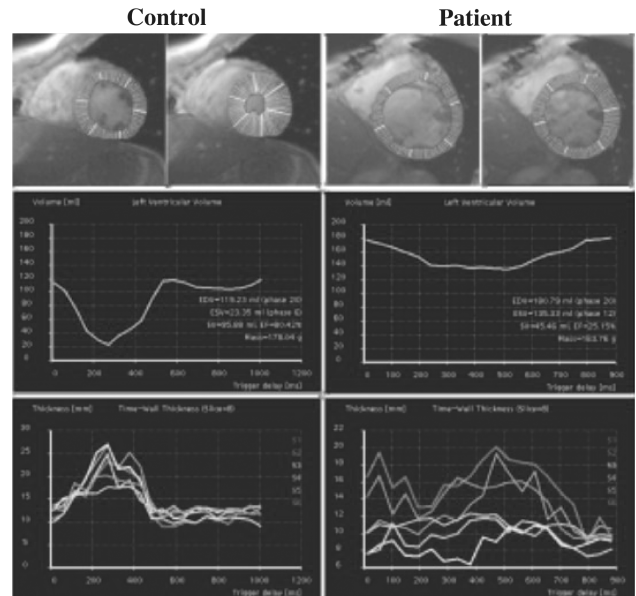


Figure 2. Normal (left) versus asymmetrical and asynchronous (right) wall motion. (View this art in color at www.dekker.com.)

Copyright © Marcel Dekker, Inc. All rights reserved.

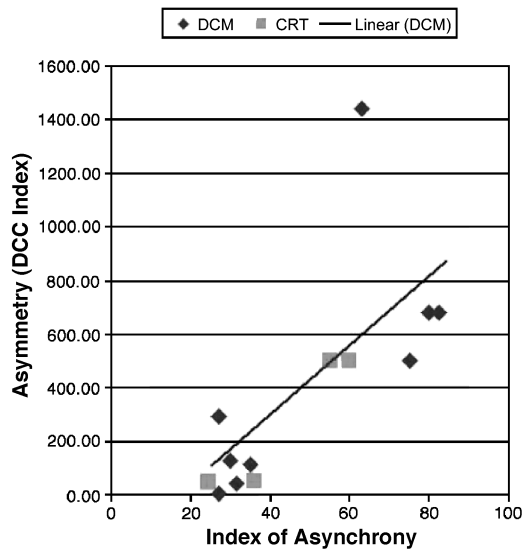


Figure 3. Correlation of asymmetry and asynchrony. (View this art in color at www.dekker.com.)

all subjects. I_a measures were on average thirty-five times higher in patients with DCM than in control subjects ($P < 0.05$). Measures of I_s and ECC also distinguished control from DCM patients ($P < 0.0005$ and $P < 0.001$ respectively). Patients qualified by current criteria for CRT were within the ranges measured in DCM patients.

Discussion: I_a % and I_a proved capable of distinguishing DCM from control. The power of I_a to determine DCC reduced from 458 (1) to 20 the number of patients required for a future trial of DCC in CRT. Inclusion of I_s (and strain) reduce the number still further as shown in Figure 3. CRT candidates were readily defined by CMR measurements of DCC.

Conclusion: 1) CMR analysis by MASS and HARP permits quantification of DCC for the individual patient. 2) Assuming that DCC is the critical component of chronic heart failure to be corrected by CRT, MR may be efficacious in screening patients to improve outcome for this valuable but costly therapy. 3) A study of the predictive value of DCC using clinical outcome (6 min. walk) after CRT is in progress.

Acknowledgments: This study was supported by grants from HMRI and RSRI. We would like to thank Dr. Richard Bing for his support and interest in this study.

REFERENCES

Abraham, W. T., et al. (2002). *NEJM* 346:1845.
 Bax, J. J., et al. (2002). *NEJM* 347:1803.
 Enriquez, C. M., et al. (2003). *ISMRM*, (Late Breaking #7).

355. Are Geometric Indices, Derived from CMR, Able to Differentiate Various Forms of Cardiac Hypertrophy?

Steffen E. Petersen,¹ Joseph B. Selvanayagam,¹ Jane M. Francis,¹ Frank Wiesmann,¹ Saul G. Myerson,¹ Matthew D. Robson,¹ Ingegerd Östman-Smith,² Barbara Casadei,¹ Hugh C. Watkins,¹ Stefan Neubauer.¹
¹Department of Cardiovascular Medicine, University of Oxford Centre for Clinical Magnetic Resonance Research, John Radcliffe Hospital, Oxford, United Kingdom, ²Division of Pediatric Cardiology, Queen Silvia Children's Hospital, Gothenburg, Sweden.

Introduction: The clinical diagnosis of hypertrophic cardiomyopathy (HCM) may be challenging when relying on echocardiography. HCM may produce a wide range of cardiac phenotypes, often making the differentiation from other causes of cardiac hypertrophy such as hypertensive heart disease (HHD), aortic stenosis (AS) or athletes' hearts (AH) difficult. Typical morphologic echo criteria for HCM are left ventricular hypertrophy (LVH), asymmetric distribution of hypertrophy, low end-systolic volumes and high ejection fractions. Cardiac magnetic resonance (CMR) provides higher image quality and is intrinsically 3D, not relying on geometric assumptions, and is thus the gold standard for cardiac volume and mass studies.

Purpose: We hypothesised that HCM can be accurately differentiated from HHD, AS and AH, based on CMR-derived measurements of LV geometry, i.e., wall thickness, degree of asymmetry, left ventricular mass, end-diastolic and end-systolic volume and ejection fraction.

Methods: 46 subjects (15 HCM, 7 HHD, 12 AS, 12 AH) underwent CMR on a 1.5 T scanner (Sonata, Siemens Medical Solutions, Erlangen, Germany). Patient selection and diagnosis of HCM, HHD and AS was based on family history, ECG and echocardiography showing moderate hypertrophy. Standard SSFP (TrueFISP) Cine imaging was performed with a short axis stack covering the complete left ventricle and two long axis views: Horizontal long axis (HLA) and left ventricular outflow tract (LVOT) view. Manual post-processing with Argus Software 2002B (Siemens Medical Solutions, Erlangen, Germany) computed left ventricular ejection fraction (LVEF), left ventricular mass index (LVMI), left ventricular end-diastolic (LVEDVI) and end-systolic volume index (LVESVI). Manual measurements of the maximal end-diastolic septal wall thickness and the minimal lateral end-diastolic wall thickness in both long axis views and the SA apical to the LVOT and basal to the papillary muscles were carried out on the Syngo 2002B software package. The maximal values of HLA, LVOT and SA



Table 1. Geometric indices in different forms of hypertrophy.

Diagnosis (N)	HCM (15)	HHD (7)	AS (12)	AH (12)
LVEF (%)	76.6±4.7	77.1±6.9	67.5±20.3	67.9±5.9
LVMI (g/m ²)	97.7±94.3	71.5±13.6	102.7±47.2	71.8±18.9
LVEDVI (ml/m ²)	78.1±15.7	71.5±11.4	79.8±35.6	93.3±9.2
LVESVI (ml/m ²)	18.5±5.8	16.7±6.4	32.7±37.3	30.1±7.1
Max WT (cm)*	2.1±1.2 [§]	1.9±0.7	1.9±0.4	1.1±0.2 [§]
DA (arbitrary units)*	2.0±0.5 [§]	1.7±0.3	1.8±0.3 [§]	1.3±0.1 ^{§,§}
Percent correct (%)	73.3	57.1	58.3	100.0

*Denotes statistical significant (p<0.05) difference within the four patient groups with left ventricular hypertrophy using one-way ANOVA. Statistically significant (p<0.05) differences are marked as [§] (HCM vs. AH), ^{§§}(AS vs. AH). Values are given as mean±standard deviation.

slice measurements were used to calculate maximal end-diastolic wall thickness (Max WT) and maximal end-diastolic septum-to-lateral wall ratios as a parameter to assess the degree of LV asymmetry (DA). Data post-processing was done blinded to the clinical diagnosis. One-way ANOVA with adjustments for multiplicity (Bonferroni) were used to compare LVEF, LVMI, LVEDVI, LVESVI, Max WT and DA in the four groups of patients. A p-value<0.05 was considered statistically significant. Multinomial logistic regression was used to predict the probability to correctly classify subjects.

Results: Table 1 shows results for LVEF, LVMI, LVEDVI, LVESVI, Max WT and DA for the four patient groups with LVH. Intra-observer and inter-observer variabilities were low. Max WT showed no difference for HHD, AS and AH, but a significant difference between HCM and AH (p=0.02). There was also a difference for the degree of asymmetry between HCM and AH (p<0.001) and between AS and AH (p=0.02), but not for the remaining LVH groups. Using multinomial logistic regression 11/15 HCM were classified correctly as having HCM (73.3%) and 12/12 AH as having AH (100%). HHD and AS could only be classified correctly in 57.1% and 58.3%, respectively.

Conclusions: HCM and AH can be discerned reliably from each other using six easily determinable geometric LV parameters (LVEF, LVMI, LVEDVI, LVESVI, Max WT, DA). This may be useful when AH needs to be differentiated from HCM when screening athletic family members with a high a priori risk of having inherited HCM and ambiguous echo results. However, the differentiation of HCM from pressure overload LVH (HHD, AS) cannot be achieved using geometric CMR parameters alone. Therefore, a multi-parametric MR approach may be needed including assessment of diastolic function, delayed enhancement to identify patchy areas of fibrosis and possibly cardiac ³¹P-Spectroscopy to further clarify the cause of hypertrophy in such patients.

356. Effect of Volumetric Imaging and Characterization of Geometry on Prevalence and Patterns of Left Ventricular Hypertrophy in the Framingham Pilot MRI Study

Michael L. Chuang, MD,¹ Daniel Levy, MD,² Carol J. Salton, BA,¹ Kraig V. Kissinger, BS, RT (R) (MR),¹ Christopher J. O'Donnell, MD, MPH,² Warren J. Manning, MD.¹ ¹Cardiovascular Division, Beth Israel Deaconess Medical Center, Boston, MA, USA, ²NHLBI's Framingham Heart Study, Framingham, MA, USA.

Introduction: Left ventricular hypertrophy (LVH) predicts excess cardiovascular morbidity and mortality. LV geometry classified by relative wall thickness (RWT) may further stratify risk (Ghali et al., 1998; Krumholz et al., 1995; Verdecchia et al., 1995). Echocardiographically, concentric geometry is defined as RWT=2PWT/EDD≥0.45, PWT=posterior wall thickness, EDD=end-diastolic dimension. Persons thus may be classified as having either: concentric hypertrophy (CH=+LVH and RWT=0.45), eccentric hypertrophy (EH=+LVH and RWT≤0.45), concentric remodeling (CR=no LVH, RWT≤0.45) or normal geometry (NL=no LVH, RWT≤0.45). Despite the increased accuracy and reproducibility of volumetric imaging, there is no widely accepted volumetric descriptor of LV geometry.

Purpose: To determine: 1) whether stratification by volumetric LV mass and RWT affects prevalence of the 4 geometric classes and 2) the effect of a novel volumetric measure, the "relative total mass" (RTM) in place of RWT on patient classification.

Methods: 278 adults (133 men, 145 women) aged 59±9 years free of clinical cardiovascular disease from the Framingham Offspring cohort underwent imaging on a 1.5-T CMR system (Philips Medical Systems, Best, the Netherlands) using an ECG-triggered breathhold cine-FFE-EPI sequence (TR=RR, TE=9 ms, FA=30°, slice



thickness=10 mm, gap=0, in-plane resolution=1.25 × 2.0 mm²) to encompass the left ventricle. Volumetric LV mass (Vol) was determined by summation of disks and RTM defined as LV mass/end-diastolic volume. Linear-geometric mass was computed using the Penn cubed formula, Penn=1.04*((EDD+IVS+PWT)³–EDD³)–13.6; IVS=septal thickness. EDD, PWT and IVS were measured from a slice just basal to the papillary muscle tips. Imaging method-specific thresholds were used to determine LVH. For volumetric mass, LVM ≥ 201.4 g, 114.0 g/m or 77.9 g/m² (men) and 134.0 g, 81.9 g/m or 74.7 g/m² (women) indicated LVH (Salton et al., 2002). Penn-mass thresholds were LVM ≥ 259 g, 143 g/m or 111 g/m² (men) and 166 g, 102 g/m or 106 g/m² (women) (Krumholz et al., 1995; Salton et al., 2002). RWT ≥ 0.45 and RTM ≥ 1.465 were considered concentric. The RTM threshold was previously determined using ROC analysis (Chuang et al., 2002). Systolic blood pressure (SBP) was measured periodically during scanning; the mean of at least 3 measurements was used. Statistical tests used Student's t test or the chi-square test at the p<0.05 level of significance.

Results: Mean SBP=149±27 mmHg. The prevalence of Penn-formula LVH was significantly greater than that of volumetric LVH for raw values (33.8 vs. 10.4%) and after indexation to Ht (36.3 vs. 11.2%) or BSA (33.8 vs. 12.9%). There was no difference in LVH prevalence after indexation; thus results are reported for raw LV mass only. The frequency of each geometric pattern is given the Table 1. Normal mass and geometry was the predominant type regardless of imaging method and geometric classification scheme. However, Penn with RWT identified eccentric LVH as the most prevalent non-normal type, while volumetric imaging and either RWT or RTM identified concentric remodeling as the most prevalent non-normal type.

Conclusion: In adults free of clinical cardiovascular disease, normal LV geometry was the most prevalent type. Traditional echocardiographic criteria identified EH as the most common non-normal type, while volumetric mass with RWT identified CR as the most prevalent non-normal type. Volumetric mass combined with a proposed volumetric criterion for LV

geometry (RTM) further increased the proportion of CR subjects. Sstratification of subjects by RWT and LV mass differs between volumetric and M-mode (equivalent) measures. This difference is accentuated with the proposed volumetric RTM criterion for LV geometry. Further work is needed to determine the prognostic value of volumetrically-determined LVH and geometry, but linear and volumetric methods do not yield equivalent classifications with respect to LV mass and geometry.

REFERENCES

Chuang, M. L., et al. (2002). *JACC* 39:368A.
 Ghali, J. K., et al. (1998). *JACC* 31:1635–1640.
 Krumholz, H. M., et al. (1995). *JACC* 25:879–884.
 Salton, C. J., et al. (2002). *JACC* 39:1055–1060.
 Verdecchia, P., et al. (1995). *JACC* 25:871–878.

357. Evaluation of Left Ventricular Mass and Function, Gadolinium Late Enhancement and Aortic Valve Area in Patients with Aortic Stenosis Before and Early After Valve Replacement Using Cardiovascular Magnetic Resonance

Almut Mahnke, MD,¹ Dudley Pennell, MD,¹ Sanjay Prasad, MD,¹ Alicia Maceira, MD,¹ Heiko Kindler, MD,² Ornella Rimoldi, MD,² Paolo Camici, MD,² Desmond Sheridan, MD, PhD.³ ¹CMR Unit, Royal Brompton Hospital, Imperial College School of Medicine, NHLI, London, United Kingdom, ²Hammersmith Hospital, Imperial College School of Medicine, NHLI, London, United Kingdom, ³St Mary's Hospital, Imperial College School of Medicine, NHLI, London, United Kingdom.

Introduction: Aortic stenosis (AS) is associated with left ventricular hypertrophy (LVH) which is an important risk factor for left ventricular failure and cardiac arrhythmias. LVH regression has previously been shown at 6 month and one year after aortic valve replacement (AVR).

Purpose: The aim of this study was to determine the relative importance of LV decompression, by assessing LVH regression early after AVR and to investigate whether left ventricular hypertrophy caused by aortic stenosis is associated with gadolinium late enhancement indicating myocardial fibrosis.

Table 1. Frequency of LV geometric type.

	%CR	%CH	%EH	%NL
Penn and RWT	9.4	10.1	23.7	56.8
Vol and RWT	14.7	4.7	5.8	74.8
Vol and RTM	26.3	7.2	3.2	63.3

Methods: Sixteen patients (pts) (age 67 ± 10 years) with moderate to severe AS and angiographically normal coronary arteries, were studied before and 4 ± 1 weeks after AVR using echocardiography to assess severity of AS and cardiovascular magnetic resonance to assess left ventricular mass index (LVMI) and function, and aortic valve area (by planimetry). Ten pts were additionally investigated for signs of myocardial fibrosis using gadolinium late enhancement technique. Eighteen sex and age matched healthy volunteers served as controls.

Results: Before surgery LVMI was significantly higher in aortic stenosis pts compared with controls (104 ± 23 vs. 72 ± 13 g/m², $p=0.006$). All pts had normal LV volumes and function (mean EF: $73 \pm 6.8\%$). Four weeks after AVR significant regression of LVMI occurred in all pts (mean diff.: -20 ± 9 g/m², $p<0.0001$), which was more evident in pts with severe LVH ($r=-0.72$, $p=0.004$). Subendocardial gadolinium hyperenhancement was seen in 3 patients and patchy mid-myocardial hyperenhancement suggestive of myocardial fibrosis was seen in only one patient. The assessment of aortic valve area by planimetry correlated significantly with the measurement of aortic valve area by transthoracic echocardiography ($r=0.79$, $p=0.002$) (Fig. 1).

Conclusion: 1) Regression of LVM after haemodynamic unloading occurs as early as 4 weeks following AVR and the decrease is linearly related to the severity of LVH. 2) Planimetric assessment of aortic valve area by CMR is a reliable tool to assess severity of aortic stenosis providing an alternative if suboptimal echocardiographic images are obtained. 3. Significant areas of myocardial fibrosis detectable by gadolinium enhancement were not seen in our patient cohort.

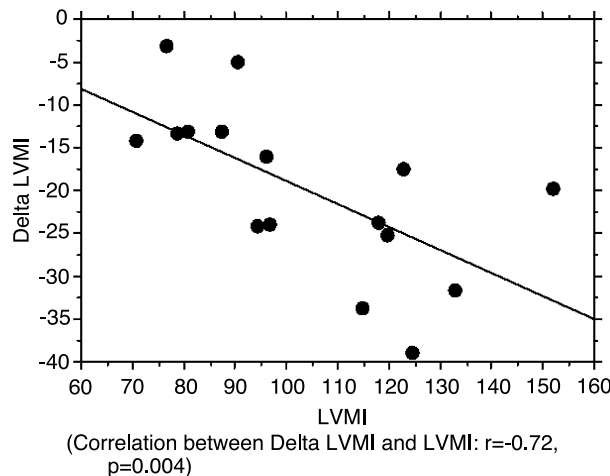


Figure 1.

358. Detection of Left Ventricular Dysfunction and Cavity Dilatation by Cardiac Magnetic Resonance and Echocardiography in Patients with Regurgitant Valvular Disease

Sean G. Hughes, MD, Thomas H. Hauser, MD, Kraig T. Kissinger, RT, Warren J. Manning, MD, Susan B. Yeon, MD. *Cardiology, Beth Israel Deaconess Medical Center, Boston, MA, USA.*

Introduction: Accurate assessment of left ventricular (LV) size and function is of particular importance in patients with mitral and aortic regurgitation. However, assessment of chamber size by 2D echocardiography (echo) requires geometric assumptions, and visual estimation of the LV ejection fraction (EF) by echo may be inaccurate, especially when the LV is dilated. Volumetric cardiac magnetic resonance imaging (CMR) is a highly reproducible method for assessing LV dimensions, volumes, and function.

Purpose: Using CMR as the gold standard, we sought to determine the sensitivity and specificity of echo for detecting LV dysfunction and dilatation in patients with regurgitant valvular disease.

Methods: We identified all patients with a clinical CMR study performed at our institution from July 2001–March 2003. Patients were included in the study population if an echo performed within 6 months of the CMR demonstrated at least moderate mitral or aortic regurgitation. Patients with segmental wall motion abnormalities were excluded. LV dysfunction was defined as an echo-EF $< 55\%$ or a CMR-EF $< 60\%$ (based on prior work at our institution identifying this as the 95% lower limit of normal). LV dilatation was defined as a LV end-diastolic dimension index (LVEDDI) of ≤ 31 mm/m² by either method, or a LV end-diastolic volume index (LVEDVI) of ≤ 81 mm/m² by CMR.

Results: Data from 20 patients meeting study criteria were analyzed. The echo-EF was significantly lower than the CMR-EF (echo-EF $54.4\% \pm 11.3\%$ vs. CMR-EF $61.8\% \pm 9.9\%$, $p<0.0001$). When modality-specific lower limits of normal were applied, the sensitivity and specificity of echo for LV dysfunction were 100% and 64%, respectively. Echo significantly underestimated the LVEDDI as compared to CMR (echo-LVEDDI 28.7 mm/m² ± 5.4 mm/m² vs. CMR-LVEDDI 34.6 mm/m² ± 4.2 mm/m², $p<0.0001$). The sensitivity of echo for LV dilatation as defined by the CMR-LVEDDI or the CMR-LVEDVI was 33% and 26%, respectively. The specificity of echo for LV dilatation was 100% by either method.

Conclusions: Compared with CMR, echo yields a lower EF and LVEDDI in patients with significant

mitral or aortic regurgitation. Echo is a sensitive test for LV dysfunction, but is not sensitive for LV dilatation. Because surgery is warranted in patients with severe regurgitant valvular disease and progressive LV dilatation, serial testing by echo alone may not be sufficient.

359. Interobserver Agreement of Delayed Gadolinium Enhanced Cardiac Magnetic Resonance Imaging in Sarcoidosis

Jan-Peter Smedema, MD,¹ Gabriel Snoep, MD,² Marinus van Kroonenburgh, MD, PhD,³ Anton P. Gorgels, MD, PhD.¹ ¹Cardiology, Academic Hospital Maastricht, Maastricht, Netherlands, ²Radiology, Academic Hospital Maastricht, Maastricht, Netherlands, ³Nuclear Medicine, Academic Hospital Maastricht, Maastricht, Netherlands.

Introduction: Sarcoidosis has been reported to cause clinical symptoms due to cardiac infiltration in 5% of patients. Postmortem studies have revealed cardiac involvement in 20–50% of cases. Echocardiography, myocardial scintigraphy and myocardial biopsy suffer from low sensitivity, low specificity or both. Delayed gadolinium enhanced cardiac magnetic resonance (CMR) imaging might be a valuable additional diagnostic technique.

Purpose: To prospectively evaluate delayed gadolinium-DTPA enhanced CMR findings in patients with various stages of sarcoidosis, determine sensitivity and specificity as compared to the guidelines for the diagnosis of cardiac sarcoidosis from the Japanese Ministry of Health and Welfare (1993) as gold standard, and determine interobserver agreement.

Methods: Breath-hold T1-weighted (with and without inversion recovery prepulse) multislice CMR examinations acquired at 1.5 T with ECG-triggering before and 10 minutes after the administration of 0.1 mmol/kg gadolinium-DTPA were performed in 51 patients with various stages of sarcoidosis. Additional evaluation included physical examination, 12 lead ECG, SAECG, 24-hour Holter ECG, echocardiography, thallium-201 and ¹²³I MIBG myocardial scintigraphy.

The presence and localization of enhancing myocardial lesions was assessed by four blinded expert observers. Interobserver variability was compared by means of a kappa statistic. The outcomes were compared with the gold standard.

Results: The range of interpreted abnormalities was variable: 7/51 to 21/51 cases. Most lesions were present in the anterolateral segments.

In 6/51 cases all observers agreed on the presence of enhancing lesions, and in 23/51 all observers agreed on the absence of enhancing lesions. In only 31/51 (61%) cases did >2 of the 4 observers agree on the presence or absence of lesions. When >2 observers agreed on the presence and >1 agreed on the absence of enhancement, the sensitivity and specificity of delayed enhanced CMR for the diagnosis of cardiac sarcoidosis according to the gold standard were 75% and 95%.

Conclusions: Interobserver agreement of delayed gadolinium-DTPA enhanced CMR in sarcoidosis was poor in our study; however with at least 3/4 observers in agreement a reasonable sensitivity for the diagnosis of cardiac sarcoidosis was reached.

360. Prevalence of Pericardial Effusion Using Cardiac MRI

Christopher K. Dyke, MD, Peter Kellman, PhD, W. Patricia Ingkanisorn, MD, Kenneth L. Rhoads, MD, Anthony H. Aletras, PhD, Anthony E. Arai, MD. *NHLBI/National Institutes of Health, Bethesda, MD, USA.*

Introduction: Pericardial effusion is a common finding during routine cardiac imaging. Free living and referral population prevalence data are limited to echo-detected effusion, but estimates using MRI have not been previously reported.

Purpose: The aim of the present study is to report the prevalence of pericardial effusion detected in a large patient population referred for cardiac MRI and to determine significant characteristics associated with the presence of MRI-detected pericardial effusion.

Methods: 832 consecutive patients who completed a cardiac MRI examination at a tertiary referral center

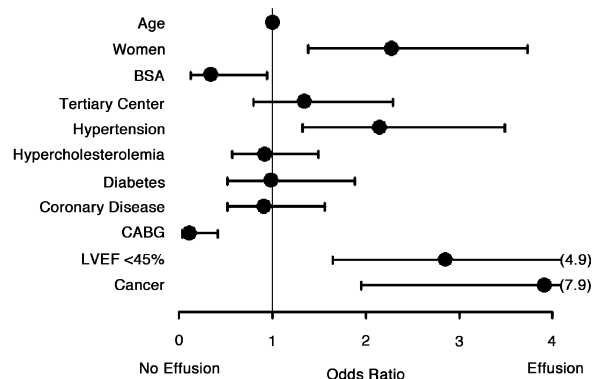


Figure 1.



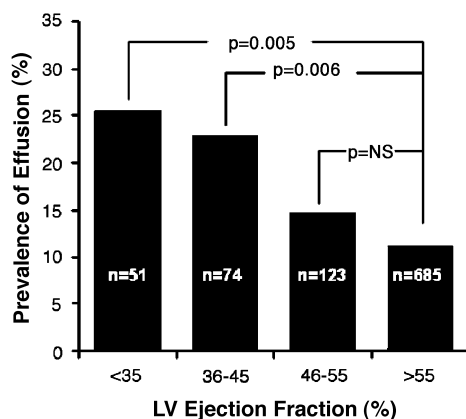


Figure 2.

(n=188) or a community hospital (n=644) were evaluated. Imaging was performed using a General Electric CV/i 1.5 T MRI system and a four-element cardiac phased array. Pericardial effusion was identified using cine Steady State Free Precession (SSFP), double inversion recovery-fast spin echo (DIR-FSE), or inversion recovery (IR). Standard echocardiographic size criteria were used to categorize the effusion as small, moderate, or large. Logistic regression was performed to assess the relationship between potential risk factors and the presence of pericardial effusion.

Results: MRI-detected prevalence of pericardial effusion was 15% (n=125) and was similar in the referral populations. Of the effusions, 75% (n=93) were small, 18% (n=23) were moderate, and 7% (n=9) were large. In the multivariate model, cancer (p<0.001), LVEF<45% (p<0.001), women (p=0.001), and hypertension (p=0.002) were significant predictors of effusion. Prevalence did not vary with age (p=0.56). Patients with prior bypass surgery had a lower prevalence of effusion (p<0.001). The odds ratio plot for effusion is demonstrated in Figure 1. The prevalence of effusion increased stepwise with progressively more severe abnormalities in LVEF (Figure 2).

Conclusions: The findings from this study represent the first prevalence estimates of pericardial effusion in a large consecutive series of patients referred for cardiac MRI examination. MRI-detected prevalence of pericardial effusion is 15% and was more common in women, a finding that compels further investigation to evaluate potential mechanisms and determine the prognostic significance of this finding. Effusion was also more common in patients with cancer, hypertension, or left ventricular dysfunction. Contrary to prior reports, no association with age was seen, possibly due to the ability of MRI to more accurately determine fat from fluid in the pericardial space.

361. Error Analysis Supports Phase Contrast MRI as a Robust Method for Evaluating Aortic Stenosis

Emily A. Waters,¹ Shelton D. Caruthers, PhD,² Samuel A. Wickline, MD.³ ¹Biomedical Engineering, Washington University in St. Louis, St. Louis, MO, USA, ²Cardiovascular Magnetic Resonance Laboratories, Washington University School of Medicine and Philips Medical Systems, Best, Netherlands, ³Cardiovascular Magnetic Resonance Laboratories, Washington University School of Medicine, St. Louis, MO, USA.

Introduction: MRI methods for assessing valvular disease, particularly phase-encoded velocity mapping, have achieved a level of accuracy comparable to the clinically used methods, transthoracic echocardiography and cardiac catheterization (Caruthers et al., In press). However, scan automation could further improve CMR patient throughput, while also improving reproducibility by reducing human error.

Purpose: As a preliminary investigation into the potential robustness of an automated system to evaluate aortic stenosis using the velocity-time integral method, we use cross-correlation methods to assess the similarity of flow patterns at different distances from the valve plane. The cross-correlation results measure the “sameness” of flow data between aortic levels, and hence indicate the extent of error that could be encountered from imaging planes being longitudinally mispositioned relative to flow profiles.

Methods: Patients with documented aortic stenosis via echocardiography were imaged using a 1.5 T MRI scanner (NT Intera CV, Philips Medical Systems). Quantitative images were obtained about the aortic valve plane using a free-breathing, retrospectively gated velocity encoding technique sensitized for flow in the through-plane direction (TR/TE/alpha=6.0 ms/2.9 ms/30°, 30 frames/heartbeat, 2 NSA, typical voxel size=1.0 × 1.3 × 9.0 mm³, typical encoding velocity 4 m/s). For quantitative flow measurements, one plane was positioned just to the aortic side of the valve at its greatest excursion toward the apex (typically end-systole). Two more planes were positioned distally parallel to this plane, offset 10 mm(+) and 15 mm(+) from its center.

Using IDLv.5.5 (Research Systems Incorporated) and Philips’ PRIDE image processing tools, translational cross-correlations were performed between the + and ++ level scans for each patient, calculated from a rectangular region of interest circumscribing the aortic lumen.

Results: The patient population comprised six mild, four mild-moderate, four medium, two medium-severe, and seven severe cases. Cross-correlation functions computed between aortic lumens on the +



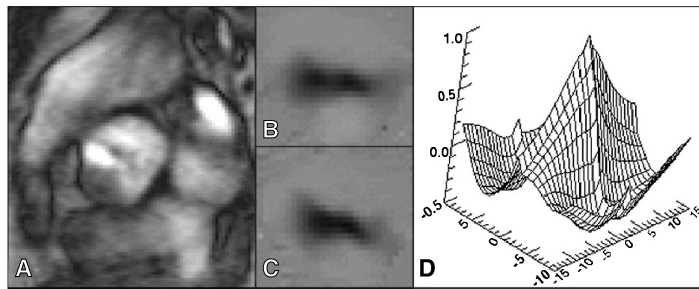


Figure 1. A) Zoomed segment of magnitude image of the aortic valve; B,C) Velocity-mapped images 1cm and 1.5cm above valve plane, respectively; D) Cross-correlation function between 1cm and 1.5cm images. Values range from 0 (white) to 1 (black). X and Y scale in pixels; note correlation peak at (0,0). Max correlation=0.99.

and ++ imaging planes had an average maximum value of 0.88 ± 0.11 (0.59–0.99). A sample analysis is shown in Figure 1. The maximum occurred at (0,0) offset for 20 of 25 patients and nonzero offset for the remaining six. In the group with zero offset, the average maximum correlation was 0.92 ± 0.07 (0.66–0.99). For the group with nonzero offset, the average maximum correlation was 0.75 ± 0.11 (0.59–0.87); echocardiographic diagnoses showed three mild, one mild-moderate, and one severe stenosis.

Discussion: A useful automated imaging system must be effective for all manifestations of the disease. A specific subgroup cannot be consistently excluded. 80% of patients representing the full range of disease exhibited a high maximum correlation with zero offset between images acquired at the + and ++ levels. The remaining 20% also spanned the full range of disease. As the majority of patients had high similarity between valve profiles at the + and ++ levels, and those with slight dissimilarities did not constitute a homogeneous subgroup, we conclude that the development of a robust method of automated slice selection should be practicable.

Conclusion: The high number of cross-correlation functions maximized at (0,0) offset indicates that there is no major qualitative change in the shape of velocity profiles between 1 and 1.5cm distal to the valve plane. This apparent insensitivity to plane location suggests that an automated slice selection algorithm would be robust against distance above the valve plane within a range of 1.0–1.5cm.

REFERENCES

Caruthers, S. D., et al. The practical value of cardiac magnetic resonance imaging for clinical quantification of aortic stenosis: comparison with echocardiography. *Circulation*. *In press*.

362. Left Atrial Volume and Ejection Fraction Assessment in Sinus Rhythm and Atrial Fibrillation Using the Biplane Area–Length Method and Cardiovascular Magnetic Resonance Imaging with TrueFISP

Burkhard Sievers, MD, Simon Kirchberg, Bodo Brandts, MD, Marvin Addo, Hans-Joachim Trappe, MD. *Cardiology and Angiology, University of Bochum, Herne, Germany*.

Introduction: Atrial fibrillation is the most common arrhythmia in elderly patients. Left atrial size and volumes play an important role in predicting the short- and long-term success rate after cardioversion.

Purpose: To determine whether cardiovascular magnetic resonance imaging (CMR) with TrueFISP and the biplane area–length method can be used for left atrial volume and ejection fraction assessment in normal subjects and patients with atrial fibrillation.

Methods: 18 healthy subjects (mean age 65.6 ± 6.4 years) and 15 patients with atrial fibrillation (mean age 67.2 ± 8.8 years) were examined using a 1.5 Tesla CMR imager. Images were acquired by TrueFISP using the horizontal and vertical long axis planes to measure left atrial end-diastolic and end-systolic area and longitudinal dimensions. Volumes were determined with commercially available software (Siemens). Left atrial end-diastolic (EDV), end-systolic (ESV), and stroke (SV) volumes and ejection fraction (EF) were calculated using the biplane method and compared with results obtained by the standard short axis method. Images were acquired and analyzed twice in the patients with atrial fibrillation.

Results: There was no difference in age between men and women ($p=0.147$) and normal subjects and patients ($p=0.128$) included in the study. EDV, ESV, and SV were significantly higher and EF significantly lower in patients with atrial fibrillation than in healthy



subjects ($p \leq 0.009$), regardless of the method used. Values for EDV and ESV obtained by the biplane area-length method in healthy subjects ($p < 0.001$) and patients with atrial fibrillation ($p < 0.001$) were significantly higher than those obtained by the standard short axis approach, whereas SV ($p \geq 0.057$) and EF ($p \geq 0.118$) did not differ significantly. In the second examination in patients with atrial fibrillation, ESV, SV, and EF did not differ significantly between the two methods ($p \geq 0.481$). The interobserver variability shows very good agreement between the measurements of the first examination in healthy subjects and patients and the second examination in patients with atrial fibrillation (overall variability 0.8+6.5%).

Conclusions: Left atrial volumes and ejection fraction can be assessed by CMR and True FISP with the biplane area-length method in normal subjects and in patients with varying heart cycle length, as in atrial fibrillation. Although the heartbeat varies in patients with atrial fibrillation, the reproducibility of the measurements is very good.

363. Quantifying Mitral Stenosis Accurately with Velocity-Encoded MRI by the “Pressure Half-Time” Method: Repeatability Study

S. J. Lin, MSEE,¹ W. Liu, MS,² M. P. Watkins, RT,¹ T. A. Williams, RT,¹ P. A. Brown, RDCS,¹ K. A. Lehr, ADN,¹ G. M. Lanza, MD,¹ S. A. Wickline, MD,¹ Shelton D. Caruthers, PhD.³ ¹Cardiovascular MR Labs, Washington Univ. School of Medicine, St. Louis, MO, USA, ²Cardiovascular MR Labs and Biomedical Engr., Washington University, St. Louis, MO, USA, ³Cardiovascular MR Labs, Washington Univ. and Philips Medical Systems, St. Louis, MO, USA.

Introduction: Mitral stenosis in adults occurs usually as a consequence of either calcific or rheumatic disease, and requires absolute quantification for appropriate medical or surgical management. Recently, velocity-encoded MRI employing the pressure half time ($P_{1/2}T$) method for quantification of mitral valve (MV) stenosis has been shown to have accuracy similar to that of ultrasound. However, if this method is to be applied ubiquitously as a clinical tool, the approach must exhibit minimal interobserver variation. Accordingly, we implemented an MRI phase contrast version of the $P_{1/2}T$ method to estimate the orifice area of stenotic MV. Two independent observers analyzed the data, which was then compared against valve sizes computed independently from Doppler ultrasound data.

Purpose: The purpose of this study is to define the extent of concordance between MV areas determined by the $P_{1/2}T$ method of velocity-encoded MRI wherein the data are analyzed by two independent observers. Furthermore, measurements of the maximum velocities across the mitral valve during early and late diastole (E_{max} and A_{max} , respectively) also were compared. In addition to interobserver comparisons, these MR results are compared against ultrasound.

Methods: Ten patients with an echocardiographic diagnosis of mitral stenosis were recruited. Each patient was imaged using a whole-body MRI unit operating at 1.5 T (Intera CV, Philips Medical Systems, Best, Netherlands). With the use of the velocity-encoded MR technique, quantitative flow images (through-plane encoding) were acquired (TE/TR/ $\alpha = 3.0$ ms/6.1 ms/30°, Matrix 128 × 256, FOV=350 mm, thk=8 mm, temporal resolution=30 phases/RR interval). The velocity-encoded MRI series were performed in the left ventricular short axis plane oriented parallel to the MV, positioned 1.5 cm from the valve plane toward the apex. The maximum encoding velocity limit (V_{ENC}) was chosen as ~2 m/s. If velocity aliasing occurred, the images were re-acquired with a higher V_{ENC} . All MR images were transferred to an offline workstation (EasyVision R5.1, Philips Medical Systems) for quantitative flow analysis and were analyzed separately by two readers in the following manner. A region of interest was drawn to include the stenotic mitral jet. The peak flow velocity through the valve measured in each phase during diastole was used as a starting point to determine the $P_{1/2}T$ by a least squares fitting technique to the linear portion of the flow velocity curves (as determined visually by the reader). E and A-wave velocities were defined (E_{max}

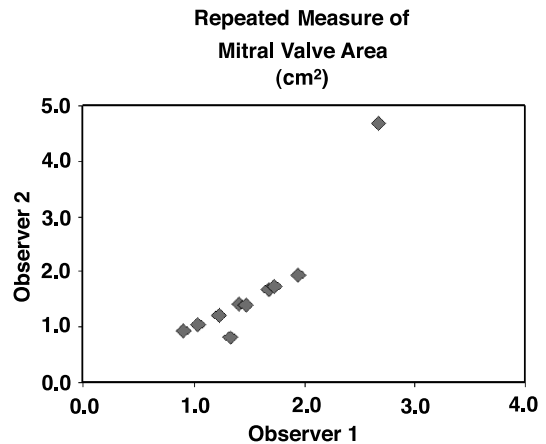


Figure 1. The mitral valve area estimated independently by two readers using the pressure half time method is highly reproducible. (View this art in color at www.dekker.com.)



and A_{max}). All MRI values were compared double-blinded with ultrasound measurements, which were recorded by a skilled sonographer and analyzed immediately with the patient remaining on the MRI trolley table. For both MRI and Doppler ultrasound, valve area was estimated as $220/(P_{1/2}T)$.

Results: Figure 1 illustrates excellent concordance between MV area analyses by different readers ($r=0.92$, $p<0.001$). The MRI valve sizes estimated by each reader also correlated well with Doppler ($r=0.92$ and $r=0.94$, $p<0.001$). In addition to MV, the component measurements of $P_{1/2}T$, E_{max} and A_{max} also correlated well between readers ($r=0.84$, $r=0.99$, $r=0.99$, $p<0.001$), suggesting that the phase contrast MR data can routinely give the correct answer.

Discussion and Conclusion: Velocity-encoded MRI is a useful and reliable tool for quantification of mitral valve areas with the use of the conventional pressure half time method. Although this method requires manual ROI identification and user-dependant interpretation, the MRI flow data analysis provides robust and repeatable estimates of the maximum velocities in early and late diastole and accurate quantification of mitral valve areas when compared to echocardiography.

364. Concentric Remodeling is Associated with a Decreased Regional Left Ventricular Function: Multi-Ethnic Study of Atherosclerosis, Substudy of Tagged MRI

Boaz D. Rosen,¹ Thor Edvardson, MD, PhD,¹ David Bluemke, MD, PhD,² Li Pan,³ Michael Jerosch-Herold, PhD,⁴ Sinha Shantanu, PhD,⁵ Shenghan Lai, MD, PhD,⁶ Joao A. C. Lima, MD.¹ ¹Cardiology, Johns Hopkins Hospital, Baltimore, MD, USA, ²Radiology, Johns Hopkins Hospital, Baltimore, MD, USA, ³Department of Medical Imaging, Johns Hopkins University, Baltimore, MD, USA, ⁴Radiology, University of Minnesota, Minneapolis, MN, USA, ⁵Radiology, UCLA, Los-Angeles, CA, USA, ⁶Department of Epidemiology, Johns Hopkins School of Public Health, Baltimore, MD, USA.

Introduction: Left ventricular concentric left ventricular hypertrophy (LVH) is a risk factor for congestive heart failure (CHF) but the transition between compensatory concentric remodeling and hypertrophy to regional and a global myocardial dysfunction has not been thoroughly defined.

Purpose: The purpose of our study was to investigate the association between concentric LV remodeling and regional LV function expressed as peak systolic

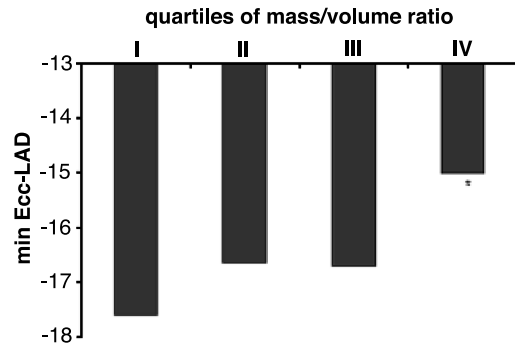


Figure 1.

midwall circumferential strain (Ecc) in participants of the Multi-Ethnic Study of Atherosclerosis (MESA).

Methods: Peak systolic Ecc from 441 tagged MRI studies was obtained by Harmonic Phase Imaging (HARP) and its relationship with the degree of concentric remodeling expressed by LV mass/ end diastolic volume (M/V) ratio was studied. Regions were defined by coronary territories: left anterior descending coronary, (LAD), left circumflex (LCX) and right coronary artery (RCA), according to recently published standards.

Results: In both genders, reduced strain was seen in the highest quartile of M/V ratio when compared to lower quartiles (-13.2 vs. -15.3 , $p<0.01$). This decrease was regionally nonuniform and was more pronounced in the left anterior descending (LAD) region (Figure 1, $*p<0.01$). However, it was statistically significant in all regions. Reductions between the first three quartiles and the fourth quartile in LAD, right and circumflex territories were 15.3%, 12.3% 10.3%, respectively ($p<0.05$ for all).

Conclusion: Concentric remodeling is associated with regional systolic dysfunction in asymptomatic individuals. This reduced function is more pronounced in the LAD territory but also present in other regions and may reflect transition from compensatory concentric remodeling to global LV dysfunction and heart failure.

365. Correlation Between Hyperenhancement on Delayed Contrast Enhanced MRI and Diastolic Function in Hypertrophic Cardiomyopathy

Munenobu Motoyasu,¹ Hajime Sakuma,² Shoko Uemura,¹ Katsuya Onishi,³ Tsutomu Okinaka,¹ Naoki Isaka,¹ Kan Takeda,² Takeshi Nakano.¹ ¹First Department of Internal Medicine, Mie University, Mie, Japan, ²Department of Radiology, Mie University, Mie, Japan,



³Department of Laboratory Medicine, Mie University, Mie, Japan.

Introduction: Diastolic dysfunction is common in patients with overt hypertrophic cardiomyopathy (HCM). However, relationship between the extent of fibrosis and impaired diastolic function in HCM patients has not been fully determined.

Purpose: The purpose of this study was to evaluate if altered diastolic function in HCM is significantly related to the extent of myocardial fibrosis demonstrated by delayed contrast enhanced MRI.

Methods: Seventeen patients (13 men, 4 women, mean age 57.7±9.8 years) with HCM were studied. The severity index of hyperenhancement on delayed contrast enhanced MRI was determined by scoring the extent of hyperenhanced tissue in 30 myocardial segments. The peak filling rate (PFR) during diastole, LVEF and LV mass were determined by using steady state cine MRI with high temporal resolution.

Results: Contrast-enhanced MRI demonstrated hyperenhancement in 97 of the 510 segments (19%) and 13 of the 17 patients (77%). The severity index determined by delayed enhanced MRI showed a strong negative correlation with the PFR ($r=-0.86$, $p<0.01$), and significant negative correlation with LVEF ($r=-0.59$, $p<0.05$). No significant correlation was observed between the severity index of hyperenhancement and LV mass ($r=0.23$, $p=0.30$).

Conclusions: The results in the current study using delayed contrast enhanced MRI and steady state cine MRI indicated that severity of myocardial fibrosis revealed by contrast enhanced MRI has a strong correlation with diastolic dysfunction in patients with HCM.

assessment of fatty infiltration, which can be achieved non-invasively with magnetic resonance imaging (MRI). Early diagnosis allows the patient to make appropriate lifestyle changes to possibly decrease the mortality of the disease.

Purpose: The standard (control) MRI protocol places the signal-generating coil directly on the anterior chest wall and produces a non-specific high intensity signal that obscures the high signal from fatty infiltration. The aim of this study was to determine whether increasing the distance between the coil and the anterior chest wall would improve identification of fatty infiltration.

Methods: Thoraces from seven embalmed cadavers were imaged on the 1.5 Tesla MRI apparatus using the control protocol and an experimental protocol with a 6 cm distance between coil and chest surface. A representative MR axial image and corresponding gross section of the heart were analyzed in each case. Fatty infiltration was graded on the MR images in the area typically affected in ARVD/C patients and correlated with histopathology of the same region.

Results: The experimental protocol was found to be more accurate in the fatty infiltration assessment of the least infiltrated as well as the most infiltrated cases. In two of the remaining four cases, the experimental protocol was equal in accuracy to the control protocol.

Conclusions: In five of the seven cases, the experimental protocol provided a correlation between MRI and histopathology that was as good as or better than the control protocol. The experimental protocol was also better in preventing false positive diagnosis in cases of minimal infiltration. Thus, the experimental protocol showed a stronger correlation with histopathology than did the control protocol.

366. Exploring a Novel Coil Position in the Magnetic Resonance Imaging of Arrhythmogenic Right Ventricular Dysplasia/Cardiomyopathy

Kelly Tung, MS,¹ Robert M. DePhilip, PhD,¹ Mark A. King, MD,² Subha V. Raman, MD.³ ¹Anatomy, The Ohio State University, Columbus, OH, USA, ²Radiology, The Ohio State University, Columbus, OH, USA, ³Internal Medicine, The Ohio State University, Columbus, OH, USA.

Introduction: Arrhythmogenic right ventricular dysplasia/cardiomyopathy (ARVD/C) is an asymptomatic cardiac disease characterized by fatty infiltration of the right ventricular myocardium and often results in sudden cardiac death. ARVD/C diagnosis includes

367. Flow Measurement in Ectatic Coronaries Using Magnetic Resonance Flow Mapping

Sophie Mavrogeni,¹ E Papadakis,¹ A Manginas,¹ K Spargias,¹ M Douskou,² I Seimenis,³ P Baras,³ S Foussas,¹ D V. Cokkinos.¹ ¹Onassis Cardiac Surgery Center, Athens, Greece, ²Bioatriki MRI Unit, Athens, Greece, ³Philips Hellas Medical Systems, Athens, Greece.

Introduction: Coronary artery ectasia (CAE) is defined as a dilatation of an arterial segment to a diameter at least 1.5 times that of the adjacent normal artery. CAE is considered as a variant of coronary atherosclerosis. A previous MI is present in 39% of patients with pure



ectasia. Slow flow in ectatic coronaries may occur even in the absence of atherosclerotic lesions.

Purpose: A direct noninvasive flow evaluation in CAE using MR-flow mapping (MR-FM).

Methods: Twelve patients with CAE and 10 controls matched for age were examined. MRI was performed with a 1.5 T Philips Intera MR scanner. Velocity-encoded MR images were acquired in a double oblique imaging plane, which was perpendicular to the ectatic or aneurysmatic segment of the coronary artery. The sequence used was a 2D, segmented k-space gradient-echo sequence. A frequency selective fat-saturation prepulse was employed. Scans were carried out with the patient free breathing using respiratory triggering and a 2D real time navigator beam for slice tracking. Retrospective ECG triggering from the QRS complex was implemented. Magnitude and phase-difference velocity-encoded images were derived using a view sharing reconstruction.

Results: RCA was ectatic in all patients, while 5 patients had also ectatic LAD. In controls, maximal flow velocity (MFV) was 18 ± 4 cm/sec for RCA and 21 ± 3 cm/sec for LAD. In patients with CAE, MFV was 12 ± 2 cm/sec for RCA and 10 ± 2 cm/sec for LAD (both $p < 0.05$ vs. controls).

Conclusions: CAE vessels are characterized by slower flow and lower velocities compared to normals. These patients can be evaluated noninvasively by MR-FM. This modality may guide further treatment, since the influence of various medications in this entity is controversial.

368. Myocardial Delayed Enhancement and Abnormal Cardiac Function in HIV-Positive Patients Who Develop the Lipodystrophy Syndrome

Brian D. Ross, MD, DPhil, FRCS, FRCP,¹ Cathleen M. Enriquez,² Kimberly Shriner, MD,¹ Jacquelyn Smillie,¹ Alexander P. Lin, BS,² Jeffrey Denham, MD,¹ Fernando Roth, MD,³ Allan Edminston, MD.⁴ ¹Huntington Medical Research Institutes, Pasadena, CA, USA, ²Rudi Schulte Research Institute, Pasadena, CA, USA, ³Foothill Cardiology, Pasadena, CA, USA, ⁴Southern California Heart Specialists, Pasadena, CA, USA.

Introduction: The successful treatment of HIV by highly active retroviral therapy (HAART) has resulted in a dramatic increase in the incidence of lipodystro-

phy/lipodystrophy syndromes (L) (Carr et al., 1998). Lipodystrophy is characterized by increases in circulating triglycerides and HDL and development of Type 2 diabetes mellitus, factors associated with increased risk of coronary artery disease (CAD) and myocardial infarction (MI). Elevated calcium scores in 5/8 HIV⁺L⁺ by electron beam tomography (EBT) (Shriner et al., 1980 unpublished) suggest need for further study.

Aims: 1) Validate cardiovascular MRI (CVMR) with delayed enhancement (DE) for identification of proven MI. 2) Screen HIV⁺L⁺ for abnormalities in myocardial viability and wall motion.

Patients and Methods: 12 male patients (7 HIV⁺L⁺, 7m, age 51 ± 11 y; 5 HIV⁺L⁻, 5m, age 50 ± 11 y) on HAART for an average of 5 years and 10 HIV⁻L⁻ controls (5 MI⁺, 4m, 1f, age 64 ± 22 y; 5 MI⁻, 4m, 1f, age 59 ± 14 y). Lipodystrophy was defined by clinical criteria of Carr et al. (Carr et al., 1998). To ensure effectiveness of DE, controls were age-matched HIV-negative with known heart disease, selected on the basis of known MI (MI⁺, N=5) or no known MI (MI⁻, N=5). **CVMR and DE**—All patients underwent CVMR in a GE LX 1.5-T system. Sequences included DE ten minutes post-intravenous Magnevist (Berlex, 0.2 mmol/kg) and tagging. Resulting images were processed with proprietary softwares, MASS and HARP. Myocardial viability was defined by hyperenhancement in left ventricular wall by two blinded, experienced readers (BR, PC). Wall motion was quantified as previously described (England et al., 2004; Lin et al., 2003).

9/12 HIV⁺ also underwent single voxel ¹H MRS of brain (PRESS TE 35 ms, white and grey matter) and skeletal IMCL (Shriner et al., 1980unpublished). Three

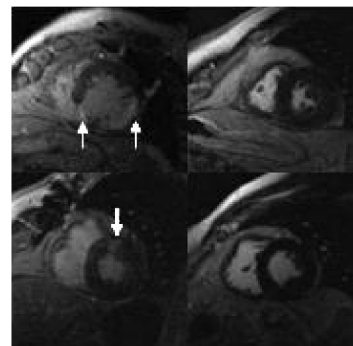


Figure 1. Top: Controls (L) HIV, positive DE, (R) HIV, negative DE patients (L) HIV L⁺, possible DE, (R) HIV L⁻, negative DE.



Table 1.

Viability	HIV-positive patients		HIV-negative controls	
	Lipo	Non-lipo	MI+	MI-
# of subjects w/enhancement	1/7	0/5	5/5	0/5

of the twelve HIV⁺ patients had EBT. All data was compared with historic controls (N=10–20).

Results: Representative cases of DE images are shown in Figure 1. DE identified nonviable myocardium in all patients with known MI (MI⁺, 5/5 positive controls) but none of the controls without MI (MI⁻; 0/5 negative controls). Only one of the HIV⁺ patients (1/7 HIV⁺L⁺; 0/5 HIV⁺L⁻) showed possible evidence of DE (Table 1). HIV⁺L⁺ and HIV⁺L⁻ did not differ significantly on the basis of left ventricular ejection fraction, stroke volume and wall thickness (Table 2). ¹H MRS distinguished HIV⁺L⁺ (reduced cerebral NAA/Cr and increased IMCL) from HIV⁺L⁻ (Table 3).

Discussion: HIV⁺L⁺ patients have several risk factors for atherosclerosis, CAD, and MI, including development of Type 2 diabetes. In accordance with

the increased risk, 3/12 patients studied had elevated EBT calcium scores, and 2/12 had cardiac symptoms sufficient to require angioplasty and stent placement. Although DE after Gadolinium was 100% effective in identifying MI in 100% of control subjects, only one of the at-risk HIV with lipodystrophy showed enhancement.

Conclusion: Prior cardiac ‘events’ necessitated stent placement in 2/7 HIV⁺L⁺ and DE in 1/7. It seems highly probable that a longer period of HAART may significantly increase cardiac risk. This pilot study established the value of CVMR with DE for earlier detection of heart risk in HIV⁺ patients who develop lipodystrophy.

Acknowledgements: Berlex for providing Magnetix for this Study. We are grateful to HMRI, RSRI and

Table 2. Cardiac measurements in an HIV-positive population.

	Lipo	Non-lipo		
N	7	5		
Sex	M	M		
Age (y)	51±11	50±11		
Weight (kg)	87±14	71±7		
Height (cm)	172±7	176±7		
BSA (m ²)	2.06±0.18	1.87±0.12		
HR (bpm)	73±11	65±10		
	Non-indexed (ml)		Indexed (ml/m ²)	
LV measures	Lipo	Non-lipo	Lipo	Non-lipo
End diastolic volume	158.79±27.19	152.47±29.81	77.19±12.65	82.42±19.78
End systolic volume	53.08±15.16	66.13±24.15	25.78±7.40	35.92±14.51
Stroke volume	105.71±20.14	86.34±8.14	51.42±9.76	46.50±6.19
Ejection fraction (%)	66.9±7.83	57.8±8.42	–	–
	Non-indexed (mm)		Indexed (mm/m ²)	
LV wall thickness	Lipo	Non-lipo	Lipo	Non-lipo
Anterior septal wall, ED	10.5±1.9	8.7±1.2	5.1±0.7	4.8±0.8
Posterior lateral wall, ED	10.0±1.6	8.2±1.7	4.9±0.9	4.4±0.9
Anterior septal wall, ES	19.0±3.4	14.7±2.7	9.2±1.6	8.0±1.7
Posterior lateral wall, ES	15.6±3.0	13.4±2.8	7.6±1.4	7.2±1.3

Table 3. Effects of lipodystrophy on brain and muscle MRS.

	HIV and lipo	HIV no lipo	p
n	8	7	
Yrs of HAART	5.0±1.6	4.7±1.4	ns
Age (y)	48±7	46±10	ns
CD ₄	247±216	546±198	0.01*
Viral load (×10 ³)	35±68	0.4±0.02	ns
Cholesterol ^a	233±70	193±31	ns
TAG _{max}	1093±779	235±159	0.01*
HDL	26±12	48±17	0.001*
IMCL/EMCL	1.91±1.4	0.92±0.4	0.05
[Creatine] _{muscle}	1.97±1.2	2.01±1.0	ns
NAA/Cr, WM	1.57±0.10	1.85±0.12	0.001*
NAA/Cr, GM	1.51±0.12	1.64±0.08	0.01

^aOn statins [n=3].

*Multivariate correlation p<0.01.

Berlex for additional financial support and Dr. Patrick Colletti for image interpretation.

REFERENCES

Carr, A., et al. (1998). *AIDS* 12:51–58.
 England, B., et al. (2004). *SCMR Barcelona* (submitted).
 Lin, A. P., et al. (2003). *ISMRM Florida*.
 Shriner, K., Edminston, A., unpublished.

369. Disparate Effects of Indexation to Fat-Free Body Mass on Gender Differences in Left Ventricular Mass

Michael L. Chuang, MD,¹ Carol J. Salton, BA,¹ Kraig V. Kissinger, BS, RT (R) (MR),¹ Christopher J. O'Donnell, MD, MPH,² Daniel Levy, MD,² Warren J. Manning, MD.¹ ¹Cardiovascular Division, Beth Israel Deaconess Medical Center, Boston, MA, USA, ²NHLBI's Framingham Heart Study, Framingham, MA, USA.

Introduction: Elevated left ventricular (LV) mass is associated with excess cardiovascular morbidity and mortality. Indexation of LV mass to height (Ht) or body surface area (BSA) is used to account for differences overall body size between individuals, but regardless of imaging method or modality used, mean

LV mass is consistently greater in men than women, and this difference persists despite indexation to Ht or BSA. However, it has been suggested that indexation to fat-free body mass (FFM) may more accurately reflect metabolic demand and thus allow more accurate identification of inappropriately elevated LV mass.

Purpose: to determine the effect of indexation to FFM on gender differences in LVM determined using volumetric cardiovascular magnetic resonance (CMR) imaging in a population of community-dwelling adults free of clinically apparent cardiovascular disease.

Methods: 144 women and 135 men from the Framingham Offspring cohort underwent CMR on a 1.5-T system (Philips Medical Systems, Best, the Netherlands). Blood pressure was measured during imaging using an automatic oscillometric device and the average of at least three measurements was used. A breath-hold cine FFE-EPI sequence (TR=R-R interval, TE=9 ms, FA=30°, in-plane resolution 1.25 × 2.0 mm²) was used to acquire 10-mm contiguous LV short-axis slices encompassing the left ventricle at end-tidal expiration. Volumetric LV mass was determined from the end-diastolic phase by summation of disks. FFM was calculated using two gender-specific methods. The Kvist formula (Kvist et al., 1988) which is based on computed-tomography measurements, estimates adipose mass as 0.923*(1.36*Wt/Ht–42.0) kg in men and 0.923*(1.61*Wt/Ht–38.3) in women, Wt=weight. Kvist-formula FFM is adipose mass subtracted from total body mass. The Kuch formula (Kuch et al., 2001), based on bioelectric impedance measures, estimates FFM as 5.1*Ht^{1.14}*Wt^{0.41} for men and FFM=5.34*Ht^{1.47}*Wt^{0.33} for women. LV mass was indexed to Ht, Wt, BSA, Ht^{2.7} (de Simone et al., 1992) and to FFM by the Kvist and Kuch methods. Data are summarized as mean±standard deviation and gender differences assessed using simple t tests. To account for possible gender differences in mean blood pressure, analyses were also performed considering only normotensive (SBP<140 mmHg) subjects.

Results: Women and men did not differ in age (60±9 and 59±9 years respectively, p=NS) but mean SBP was lower in women (146±26 vs. 153±28 mmHg, p=0.04). For the 64 women and 41 men with SBP≤140 mmHg mean SBP did not differ (124±12 vs. 121±12, p=0.22). “Raw” (non-indexed) and indexed masses by gender are shown in the Table 1. For the study group as a whole, men had significantly greater raw mass and this difference persisted after indexation to Ht, Ht^{2.7}, BSA and Wt. Indexation to Kuch-FFM eliminated gender differences in LV mass, while indexation to Kvist-FFM revealed significantly

Table 1. Raw and indexed LV mass by gender.

Index	None	Ht	Ht ^{2.7}	BSA	Wt	Kvist	Kuch
Men	156±29	88±16	33±6.5	76±14	1.8±0.36	2.42±0.43	2.55±0.46
Women	110±20	62±14	30±6.4	63±10	1.6±0.29	2.68±0.51	2.51±0.44
p-value	<0.001	<0.001	<0.001	<0.001	<0.005	<0.005	0.45, NS

greater adjusted LV mass in women than in men (p<0.001). These relationships were consistent when considering only normotensive subjects, apart from indexation to Ht^{2.7}, after which gender differences marginally crossed into non-significance with p=0.054.

Conclusion: Men have greater ‘raw’ LV mass than women and this gender difference persists after indexation to anthropomorphic descriptors including Ht, Ht^{2.7}, Wt and BSA. However, indexation to calculated FFM eliminates gender differences in mean LV mass using an estimator (Kuch) derived from bioelectric impedance measures, and actually reveals greater indexed LV in women compared to men with using an imaging-based estimator of FFM. Further work is needed to determine the prognostic value of LVM indexed to calculated FFM.

REFERENCES

de Simone, G., et al. *JACC* 20:1251–1260.
 Kuch, B., et al. *J. Hypertens.* 19:135–142.
 Kvist, H., et al. *Am. J. Clin. Nutr.* 48:1351–1361.

370. Assessment of Aortic Stenosis with Cardiovascular Magnetic Resonance

Begoña Igual, MD,¹ Alicia M. Maceira, MD,¹ Vicente Miró, MD,² Pilar López-Lereu, MD,¹ Joaquín Martín,¹ Jordi Estornell,¹ M Arnau, MD,² Miguel Palencia, MD.² ¹Eresa, Hospital La Fe, Valencia, Spain, ²Department of Cardiology, Hospital La Fe, Valencia, Spain.

Introduction: Phase contrast (PC) cardiovascular magnetic resonance (CMR) sequences allow for the accurate assessment of aortic stenosis (AS). Currently, its clinical utility is limited and thus the use of these sequences is scarce.

Purpose: Our aim was to analyse the results of this technique in the assessment of AS severity com-

pared to those derived from echocardiography, and also to evaluate the utility of aortic planimetry in the study of AS.

Methods: 30 consecutive patients with known aortic valve disease referred for a CMR study to assess ascending aorta dimensions between January and April 2003 were included. The studies were performed with a General Electric[®] CVI (1.5 T) scanner. All of them underwent Doppler-echocardiography scan within 2 weeks. The study protocol included: 1) multislice dark blood (SSFSE) sequence in transverse orientation of the thorax to provide an overview of the cardiovascular anatomy, 2) FIESTA cine VLA, four-chamber and short-axis images to measure left ventricular mass and ejection fraction and 3) vascular PC sequences in three transverse planes across the aortic valve from which aortic valve area (AoVA) and peak velocity (AoPV) were obtained. regurgitant orifice (RO, mm²) and regurgitant fraction (RF,%) were obtained. CMR criteria of AS severity: mild if AoPV<3 m/s, moderate if 3 m/s<AoPV<4 m/s and severe if AoPV>4 m/s.

Results: Mean age was 65±11 yrs, 21 males. In 11 cases (37%) the aortic valve was bileaflet. Pure aortic stenosis was found in 6 patients (20%), pure AR in 11 subjects (37%) and both aortic stenosis and regurgitation in another 13 (43%). CMR and Doppler-echocardiography showed good concordance in detection of significant AS (Kappa=0.73, P<0.01). Both methods showed good correlation for calculation of EF (r=0.73, p<0.01). CMR allowed for planimetry of the AoVA in systole (see Table 1).

Conclusions: 1) Vascular phase contrast CMR sequence is a good method for evaluation of AS severity, with good concordance with Doppler-echocardiography. 2) CMR planimetry of the aortic valve

Table 1. AoVA according to AS severity.

	Mild AS	Moderate AS	Severe AS	P (ANOVA)
AoPV (m/s)	<3	3–4	>4	–
AoVA (cm²)	3.2±1	1.6±0.6	1±0.3	<0.001

area provides an objective measurement of AS severity, it is easy and simple to obtain, and it should be done routinely in the CMR assessment of aortic stenosis.

371. T2-Weighted Magnetic Resonance Imaging Detects Myocardial Edema in Acute Myocarditis

Ralf Wassmuth, Philipp Boyé, Daniel Messroghli, Rainer Dietz, Matthias G. Friedrich. *Franz-Volhard-Clinic, Humboldt-University Berlin, Berlin, Germany.*

Introduction: Myocardial edema is a feature of tissue inflammation. Whereas contrast-enhanced cardiac magnetic resonance imaging (CMR) is known to detect acute myocarditis, the diagnostic value of non-contrast CMR approaches such as T2-weighted imaging to visualize myocardial edema is not well defined.

Purpose: We assessed the signal intensity in T2-weighted images of patients with clinically proven myocarditis.

Methods: We scanned 42 healthy volunteers (18–46 years) using the body coil of a 1.5 T clinical scanner. A normal history, physical examination, ECG and echo ruled out cardiac disease. They were compared to 23 patients (16–51 years) with acute myocarditis (defined by acute onset of heart failure, history of infection, positive troponin, increased CRP or WBC, ECG-changes, normal angiography, no infarction scar in delayed enhancement). We acquired 2 short axis slices with a breathhold triple-inversion-T2-weighted black blood fast spin echo sequence (TR=2RR, TE 6,4 ms, TI 140 ms, Matrix 256 × 256, FOV 38 cm). Two independent observers read the images in random order blinded to subject identity and history. We measured signal intensity in myocardium and skeletal muscle in the same image and calculated a ratio to adjust for effects related to heart rate. The results were given in mean ± standard deviation and compared using student's t-test.

Results: Skeletal muscle signal intensity did not differ between patients and controls (38 ± 10 vs. 38 ± 7 p=ns), whereas myocardial signal intensity was higher in acute myocarditis than in controls (78 ± 26 vs. 62 ± 19, p < 0.01). The mean ratio of myocardial over skeletal muscle signal intensity was 2.2 ± 0.8 in patients versus 1.7 ± 0.6 in controls (p = 0.01). The correlation coefficient for interobserver variability was r = 0.67.

Conclusions: Mean myocardial signal intensity is increased in acute myocarditis as compared to controls.

It may have potential to corroborate the diagnosis. Due to considerable variability, it seems useful only as an additional but not as the sole parameter to establish the diagnosis of acute myocarditis.

372. Clinical Value of Cardiovascular Magnetic Resonance in the Diagnostic Workup of Patients with Suspicion of Arrhythmogenic Right Ventricular Dysplasia

Juan Sanchez-Rubio, MD, Francesc Carreras, MD, Ruben Leta, Eva Guillaumet, Sandra Pujadas, Xavier Viñolas, Guillem Pons-Llado. *Cardiology, Hospital Sant Pau, Barcelona, Spain.*

Purpose: Retrospective analysis of the usefulness of Cardiovascular Magnetic Resonance (CMR) in the assessment of patients with clinical suspicion of arrhythmogenic right ventricular dysplasia (ARVD).

Methods: CMR studies were reviewed from 46 consecutive patients (25 men aged 11–73; mean: 41 years) submitted to rule out ARVD. All exams included transaxial Spin-Echo T1w sequences for the assessment of fatty infiltration of the right ventricular (RV) wall, and Cine-MR Gradient-Echo sequences on longitudinal and short-axis planes of the heart for morphological and functional studies of the RV. Abnormal CMR findings were classified according to the general imaging criteria for the diagnosis of ARVD: Major Criteria (MC): 1) severe global dilation and reduction of ejection fraction (EF) of the RV, with preserved left ventricular (LV) EF, 2) localized aneurysm of the RV wall, 3) severe segmental dilation of the RV, 4) fatty infiltration of the RV wall; Minor criteria (mC): 1) mild global dilation and reduction of EF of the RV with preserved LVEF, 2) mild segmental dilation of the RV; 3) segmental RV wall hypokinesia.

Results: All CM studies were considered as interpretable. A normal exam was reported in 22 patients (48%), while in 24 (52%) some abnormal finding was present, either a MC or a mC, or both: 6 patients presented with 1 mC, 5 had 2 mC, 10 patients had 1 MC, 2 exhibited 1 MC+2 mC, and 1 patient had 2 MC+3 mC. Among the whole study group of 46 patients, only 5 were finally diagnosed of ARVD from clinical and electrophysiological data, all of them presenting with at least 1 MC on CMR. Fatty infiltration was observed in 9 patients on the whole group, being an



isolate finding in 6 of them while in 3 it was associated to RV wall systolic dysfunction, these later 3 patients corresponding to the group with confirmed ARVD.

Conclusions: 1) CMR exams can be performed by means of a simple study protocol in patients with suspicion of ARVD, which is readily interpretable in 100% of cases. 2) Normal studies are found in 48% percent of such patients, which permits to rule out the diagnosis. 3) Only in 21% of patients with abnormal CMR findings the clinical diagnosis of ARVD is finally confirmed, all of them presenting, however, with at least 1 MC at the CMR study. 4) The presence of fatty infiltration of the RV wall does not mean per se the presence of ARVD unless when associated with segmental abnormalities of the RV function.

373. Assessment of Pulmonary Vein Anatomy by High Resolution 3D-MRA Prior to and After High Frequency Ablation or Isolation

Andreas Tausig, MD,¹ Karin Schreiber, MD,² Hubertus Buelow, MD,² Martin Karch, MD,³ Carl Ganter, PhD,¹ Ernst Rummeny, MD, PhD.¹ ¹Dept. of Radiology, TU-Munich, Muenchen (Munich), Germany, ²Dept. of Nuclear Medicine, TU-Munich, Muenchen (Munich), Germany, ³I. Med. Clinic, TU-Munich, Muenchen (Munich), Germany.

Introduction: Pulmonary vein (PV) isolation is an effective procedure to cure resistant atrial fibrillation, but it may lead to PV-stenoses after treatment. Because of the large interindividual variation in PV-anatomy it is important to know the exact anatomical situation for optimal planning of this invasive procedure.

Purpose: Thus the purpose of this study was to evaluate if a high-resolution 3D-MRA can reproducibly identify PV-anatomy and detect iatrogenic stenosis after treatment.

Methods: Ten patients (3f, 7m; 53±7,8 yrs) were examined prior to PV-intervention and 3 pts (1f, 2m; 58±6,5 yrs) afterwards. MR imaging was performed at a 1.5 T (Sonata, Siemens) using a contrast enhanced (Magnevist 0.2 mmol/kg at 3 ml/s) breath-hold FLASH-3D-MRA pulse sequence (GRAPPA, Voxel size 1.0×0.8×1.0 mm; TA 16 s). Conventional PV-angiography served as a standard in all pts. Three independent and with respect to the results of the PV-angiograms blinded readers (R1, R2, R3) evaluated the 3D-MRA with a dedicated software package. Number of PV-ostia, number and location of PV-stenoses and the maximal diameters of the PV were reported.

Results: The 7 known PV-stenoses in 3 pts were properly identified by all readers. Two of the three observers detected the same number of PV-ostia (2×3 ostia, 10×4, 1×5); one observer judged an early branching of a PV as two separate ostia (2×3 ostia, 9×4, 2×5). Normal anatomic variations of the PV were called stenotic by R1 in 1 pt, by R2 in 2 pts and by R3 in 3 pts prior to intervention. Compared to the upper PVs, the measured mean diameters of the lower PVs were smaller. Upper PV: R1 1.7 cm, range 1.4–2.3 cm; R2: 1.9 cm, range 1.5–2.4 cm; R3: 1.7 cm, range 1.3–2.1 cm. The mean difference among them was calculated to be 0.3±0.1 cm, range 0.2–0.4 cm.

Conclusions: Contrast-enhanced high-resolution 3D-MRA is an adequate technique to visualize PV-anatomy. Furthermore it is a reliable tool to depict iatrogenic stenoses after high frequency isolation or ablation. The number of false positive stenotic findings stresses the need for serial MRAs, prior and after this treatment, in order to differentiate physiologic narrowing of a vessel from an iatrogenic stenosis.

Request Permission or Order Reprints Instantly!

Interested in copying and sharing this article? In most cases, U.S. Copyright Law requires that you get permission from the article's rightsholder before using copyrighted content.

All information and materials found in this article, including but not limited to text, trademarks, patents, logos, graphics and images (the "Materials"), are the copyrighted works and other forms of intellectual property of Marcel Dekker, Inc., or its licensors. All rights not expressly granted are reserved.

Get permission to lawfully reproduce and distribute the Materials or order reprints quickly and painlessly. Simply click on the "Request Permission/Order Reprints" link below and follow the instructions. Visit the [U.S. Copyright Office](#) for information on Fair Use limitations of U.S. copyright law. Please refer to The Association of American Publishers' (AAP) website for guidelines on [Fair Use in the Classroom](#).

The Materials are for your personal use only and cannot be reformatted, reposted, resold or distributed by electronic means or otherwise without permission from Marcel Dekker, Inc. Marcel Dekker, Inc. grants you the limited right to display the Materials only on your personal computer or personal wireless device, and to copy and download single copies of such Materials provided that any copyright, trademark or other notice appearing on such Materials is also retained by, displayed, copied or downloaded as part of the Materials and is not removed or obscured, and provided you do not edit, modify, alter or enhance the Materials. Please refer to our [Website User Agreement](#) for more details.

[Request Permission/Order Reprints](#)

Reprints of this article can also be ordered at

<http://www.dekker.com/servlet/product/DOI/101081JCMR120028314>